

PhD
CERENA
day


Book of Posters

PhD CERENA day



January 22nd, 2026

Campus Alameda, Instituto Superior Técnico, Lisboa
South Tower QA1.1

- 10:30** Welcoming Session
- 10:40** 'Handling uncertainties: from first-year doubts to a research identity with my experience at CE Roberto Miele (UNIL)
- 11:20** PhD Pitch Session
- 12:30** Lunch @ Geosciences Museum DER
- 14:00** PhD Pitch Session
- 15:00** Guided tour through CERENA's Lab
- 16:00** Meeting between PhD students and CERENA Board
- 17:00** Social Event

Index

1. **Sofia Fernandes** - Er and Er/Yb Doped TiO₂ Solar-Light-Active Photocatalysts for Minocycline Removal from Water
2. **António Mariquito** - Eco-friendly and Health-conscious Engineering of Thermally Expandable Microcapsules
3. **Marta Lourenço** - Sustainability-by-Design through Oil-Phase Selection and Recovery in the Synthesis of MICROSCAFS®
4. **Lucas Marcelino** - Biodegradable microcapsules as a pathway to microplastic-free agrochemical formulations
5. **Heithor Queiroz** - From Pruning to Harvest: Evaluating Proxy Consistency in Smallholder Semi-Arid Vineyards
6. **Bruno Camilo** – Preliminary data on long bone histology of *Eousdryosaurus* sp. (Ornithopoda: Dryosauridae) from the Upper Jurassic of Portugal
7. **Roberta Lobarinhas** - Scars from a fire: Assessing Vulnerability and Performance
8. **João Senra** - Fire as a risk and a resource to the pre-historic artists: Through the lens of Geosciences
9. **Miguel Vitoriano Teixeira** - Intelligent Management of Indoor Air Quality in GLAMs
10. **Tomás Tavares** – Green Hydrogen Production in Cape Verde from Renewable Energy Sources
11. **Shahmir Noshervani** – Technoeconomic impact of impurities on CO₂ injection in EOR and Geo-storage
12. **Rafaela Marques** - CO₂ valorisation with earth abundant metals: from bench to pilot
13. **Xiaodong Guo** - Exploring the pore structure of coal at the microscale
14. **Jakub Skiba** - Multidimensional stochastic mine planning and design for sustainable mining
15. **Olufe Oludare Joseph** – AI Applications for Prediction of Deep Underground Mine Excavation Instability - a Comparative Study to Geomechanical and Numerical Modelling Methods
16. **Amir Afzali** - Enhanced tailing modelling, characterization, and exploration
17. **Tiago Silva** - Technosol from mining tailings
18. **Arij Ben Hassine** - Hydroconversion of advanced non-conventional feedstock: impact of co-processing
19. **Salma Dehhaoui** - Sol–Gel Synthesis and Catalytic Performance of ZR-P Catalysts
20. **Maria Teresa Nogueira** - Total Plastic Recycling – Hydrocarbons and Beyond Contributions to the Circular Economy
21. **Ana Raquel Gonçalves** - Bio-oil from Biomass: Mapping Fuels to Forest Management
22. **Rita Seródio** - Performance, prediction and optimization of green hybrid composites for additive manufacturing in industrial applications: experimental and machine learning (ML) studies
23. **Sofia Aparício** - Dissolving the Problem: Plastic Recycling using Natural-Based Solvents
24. **João Galvão** – Using BELLHOP3D to understand underwater acoustics and generate artificial data
25. **Bárbara Fonseca** - Geomathematical Assessment of Environmental Degradation in Abandoned Mining Areas

Er and Er/Yb Doped TiO₂ Solar-Light-Active Photocatalysts for Minocycline Removal from Water

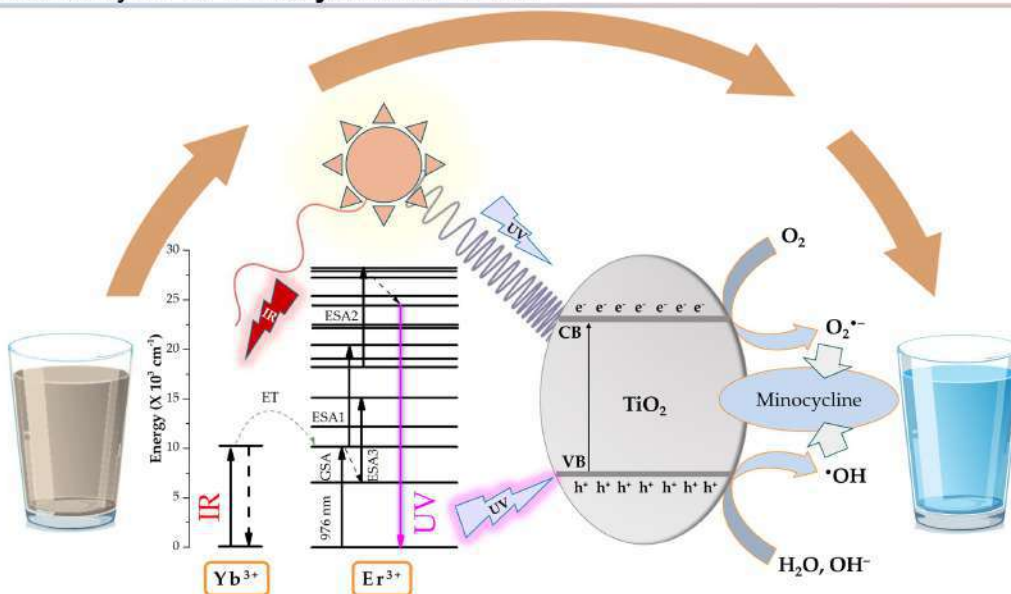
PhD in Materials Engineering

Sofia Moreira Fernandes (sofia.moreira.fernandes@tecnico.uslbova.pt)

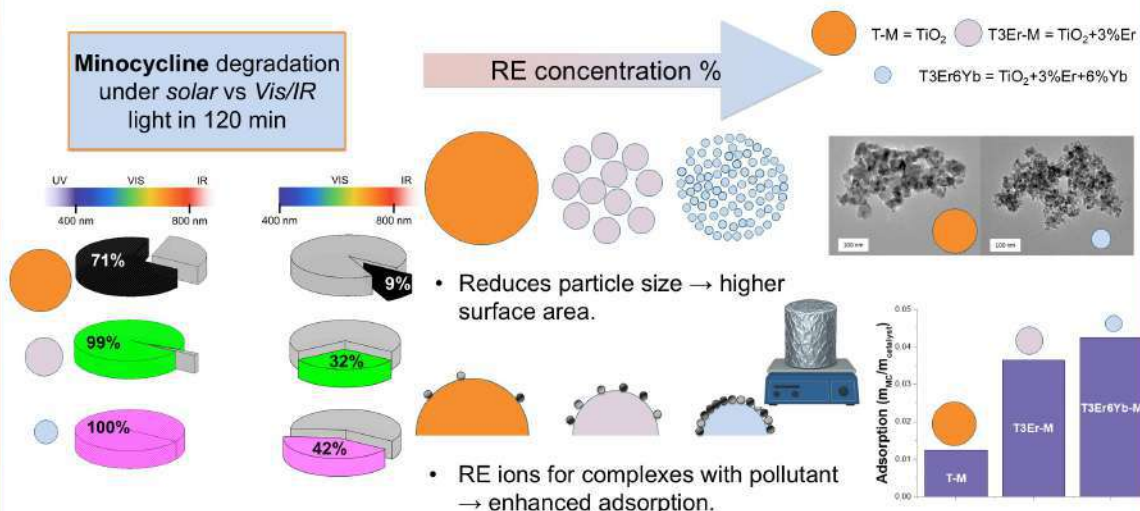
Supervisors: Ana C. Marques, Luís Santos, Markus Niederberger

INTRODUCTION

- TiO₂ is limited to UV light and suffers fast electron-hole recombination, **restricting solar-driven antibiotic degradation**.
- **Rare-earth (RE) doping** can tune TiO₂ structure and electronic properties, **enhancing light absorption and surface reactivity**.
- **Microwave-assisted RE doping** offers rapid, uniform synthesis, overcoming slow, energy-intensive conventional methods and enabling scalable photocatalysts for **minocycline removal**.



Minocycline degradation under solar vs Vis/IR light in 120 min



CONCLUSIONS

- RE doping yielded smaller TiO₂ nanoparticles with **higher specific surface area**, increasing the number of accessible active sites.
- RE ions promoted **minocycline adsorption** and enabled **IR → UV upconversion**, extending TiO₂ activity beyond the UV range.
- These effects resulted in superior solar photocatalysis, with T-3Er6Yb-M showing the highest minocycline removal efficiency.

Eco-friendly and Health-conscious Engineering of Thermally Expandable Microcapsules

Chemical Engineering

António Mariquito (antonio.mariquito@tecnico.ulisboa.pt)
Supervisor: Prof.^a Ana Clara Marques

Context

Over the past decade, industry has increasingly emphasized sustainability through improved energy efficiency and reduced carbon emissions. **Thermally Expandable Microcapsules (TEMs)**—polymeric capsules containing a volatile propellant that expands upon heating—are key blowing agents for producing lightweight materials, particularly foams. Their use lowers polymer consumption and environmental impact. Traditionally, TEMs are produced via free-radical polymerization of toxic acrylate monomers, notably nitrile-based ones such as acrylonitrile (ACN) and methacrylonitrile (MACN), which provide low gas permeability, low glass-transition temperature, and good ductility. However, health concerns have intensified: **ACN is now classified by the EU as a category 1B carcinogen** with strict exposure limits, while MACN, though not classified as carcinogenic, also poses occupational risks. **This PhD project aims to develop ACN- and MACN-free TEMs using safer, sustainable (biobased and/or biodegradable) alternatives.** The resulting formulations, spanning expansion temperatures from 60 to 220 °C, will be evaluated as foaming agents in biobased and/or biodegradable polymer matrices using processing routes such as extrusion foaming.



Figure 1: Schematics regarding the overall purpose of the thesis

TEMs with Low-Expansion Temperatures

Vinyl acetate was selected as the **soft-segment monomer** for TEMs with **low activation temperatures (≤ 65 °C)** due to its intrinsically low glass transition temperature (Tg) and favorable safety profile. In a first stage, copolymerization with higher Tg ("hard") monomers was performed as a materials-design strategy to modulate **shell stiffness and expansion behavior.**

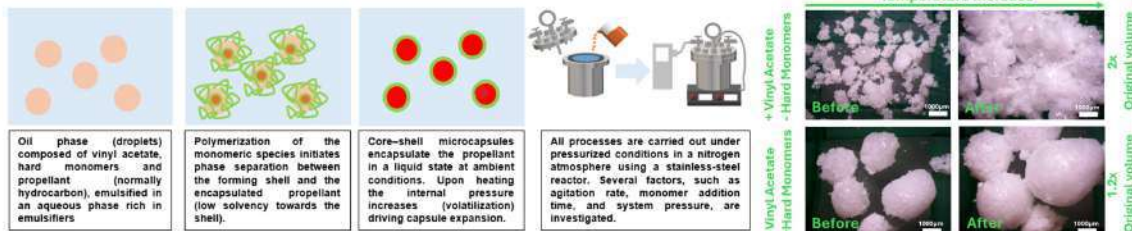


Figure 2: Schematics regarding the emulsion polymerization process of vinyl acetate based TEMs in pressurized system (between 0.1 to 1 bar) that occurs in steel reactors

Figure 3: Effect of monomer composition on the expansion behavior of the obtained TEMs at 60°C

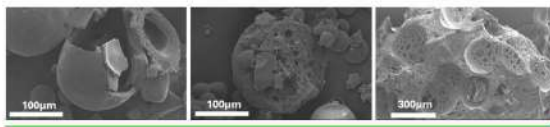


Figure 4: SEM images demonstrating shell heterogeneity and loss of core-shell structure

Hard Monomers Content	Cp 1st Tg (J/g·°C)		Cp 2nd Tg (J/g·°C)	
	1st Tg (°C)	2nd Tg (°C)	1st Tg (°C)	2nd Tg (°C)
+	0.456	38.20	-----	-----
+	0.247	40.83	0.097	69.17
+	0.129	41.24	0.084	72.51
-	0.079	42.67	0.075	76.79

Figure 5: Increasing the content of hard monomers in the synthesis leads to the appearance of a second Tg

TEMs with Low-Expansion Temperatures & Improved Biodegradability

In a second step, the most promising synthesis (+Vinyl Acetate, - Hard monomers) was further modified to produce TEMs with comparable performance while enhancing biodegradability. **This was achieved by introducing approximately 10–20 wt% of a biodegradable polyester chains derived from cyclic ester monomers.**

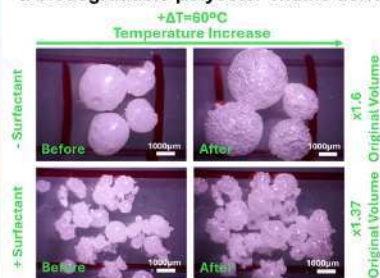


Figure 6: Increasing surfactant decreases particle size and encapsulation efficiency, incorporation of polyester chains leads to lower expansion (x2 to x1.6)

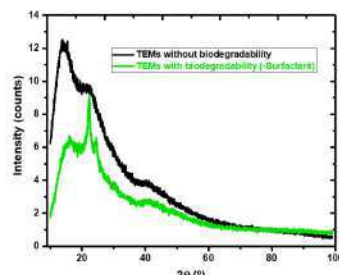


Figure 7: The appearance of the diffraction peak indicates the presence of crystalline domains promoted by the incorporation of polyester chains in the original synthesis

Conclusion

- Vinyl acetate is a successful precursor for TEMs with low expansion temperatures.
- Copolymerization with hard monomers induces shell heterogeneity due to kinetic effects.
- A partially biodegradable formulation shows increased crystallinity improving propellant retention.

Acknowledgements: This research was funded by FCT (Fundação para a Ciência e Tecnologia) under the scholarship 2024.06629.BD, Strategic Project FCT-UIDB/04028/2025 and FCT-UIDP/04028/2025

Sustainability-by-Design through Oil-Phase Selection and Recovery in the Synthesis of MICROSCAFS®

Doctoral Program in Chemical Engineering

Marta Costa Lourenço (martaclourenco@tecnico.ulisboa.pt)

Supervisor: Ana Clara Marques

Introduction

MICROSCAFS® are silica-titania microspheres with interconnected macroporosity obtained through a sol-gel polymerization-induced phase separation method. Their unique combination of chemical, thermal and mechanical robustness and tunable porosity makes them attractive for advanced applications, ranging from catalysis to biomedical and environmental remediation technologies.

To address the growing demand for sustainable materials and processes, efforts must be directed towards **greener synthesis strategies**. In this work, we propose two distinct approaches to further improve the sustainability of the MICROSCAFS® synthesis:

- **Full replacement** of the organic solvent decalin (decahydronaphthalene) with a more sustainable alternative (e.g., limonene), a bio-based and less toxic solvent obtained from citrus waste).
- **Recovery and reuse** of decalin through phase separation, thus extending the solvent's life cycle and reducing waste.

Table 1. Main properties of decalin and limonene.

Properties	Decalin	Limonene
Chemical structure		
Density (g/cm ³ , at 25°C)	0.896	0.841
Boiling point (°C)	-196	-176
Solubility in water	Insoluble	Insoluble
Refractive index	1.481	1.473
Surface tension (dyn/cm, at 20°C)	~28.5	~ 30
Viscosity (cP, at 20°C)	1.788	0.846
Toxic	Yes	No
Renewable	No	Yes

NOTE: The lower viscosity increases the risk of emulsion instability and structural defects!

Methodology

MICROSCAFS® conventional synthesis



Full replacement of the oil phase decalin with limonene

Recovery and reuse of decalin

Each implemented strategy occurs at a different stage of the process

Results

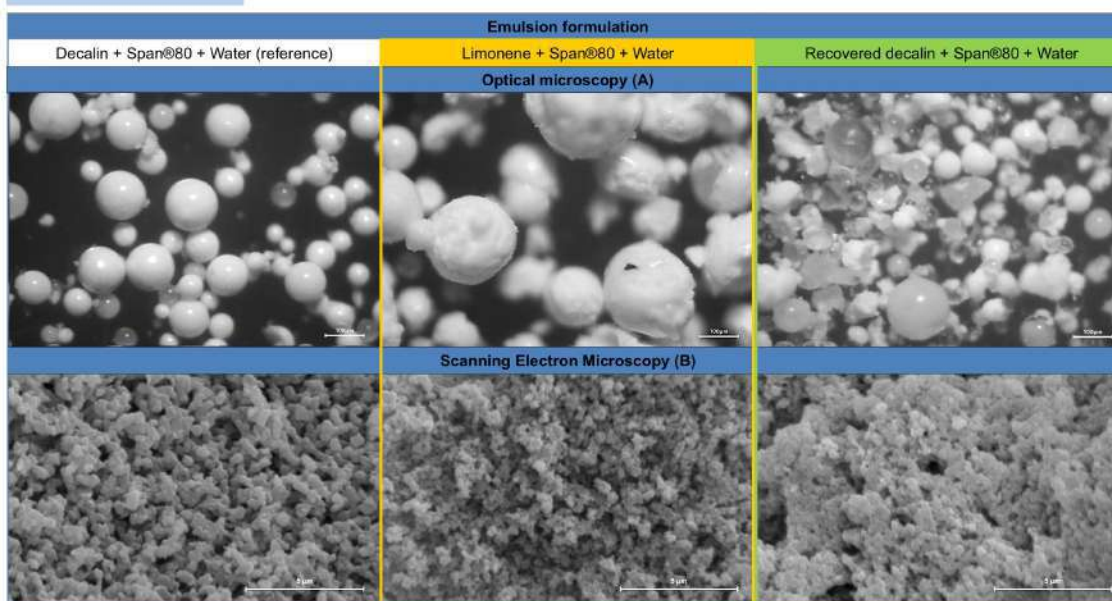


Figure 1. Characterization of the different MICROSCAFS® through: (A) optical microscopy (spheres) and (B) SEM (spheres' internal cross section).

Conclusions

Optical microscopy images show the formation of spherical particles, while SEM images reveal an internal porous structure comparable to that of the reference synthesis. Overall, these results confirm that both alternative synthesis routes are effective, although further optimization is needed to fully exploit their potential.

Acknowledgements

The authors gratefully acknowledge the support of CERENA, Strategic Project FCT-UIDB/04028/2025 and FCT-UIDP/04028/2025, and Talent Pass, Grant Agreement No. 10121448 – HORIZON-WIDERA—TALENTS-03.

Biodegradable microcapsules as a pathway to microplastic-free agrochemical formulations

Materials Engineering

Lucas P. Marcelino (lucas.marcelino@tecnico.ulisboa.pt)

Supervisors: Ana C. Marques, António Aguiar and Sónia Aparício

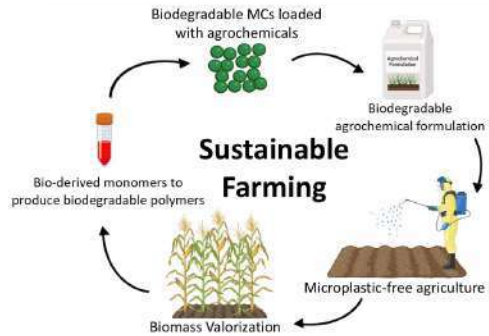
Introduction

Commercial agrochemical formulations containing microcapsules are primarily based on non-biodegradable materials such as **polyurethane** and **polyurea** leading to the spread of microplastics into our ecosystems.

The agricultural sector is one of the sectors that creates more microplastics. Capsule-suspended products, account for **500 tonnes of microplastic** used each year in the European Economic Area.

The European Commission (**September 2023**) established a **deadline of 5 years** to replace the current marketed products with microplastic-free alternatives.

Our goal is to provide an **eco-friendly solution** by encapsulating agrochemicals using **biodegradable** and **bio-based** polymers and, more sustainable agricultural practices will emerge;

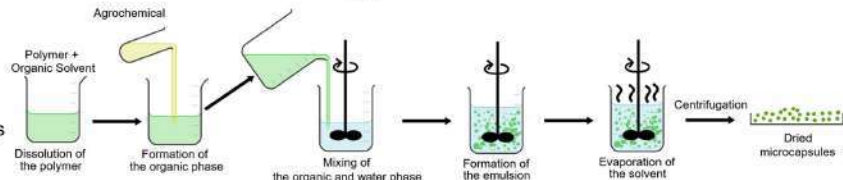


Methodology

Solvent Evaporation

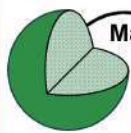
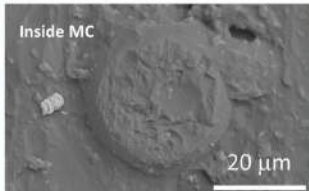
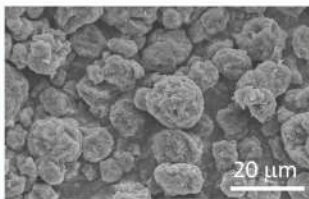
Benefits:

- Versatile
- Tunable size and loading
- Use of biodegradable polymers
- Industrially scalable



Results

SEM



Matrix-type MCs

Agrochemical dispersed uniformly throughout the polymeric matrix

Encapsulation efficiency: 97.5%

Loading: 70 wt%

Median size: $___ \mu\text{m}$

DSC

Decrease in the melting point of the polymeric matrix with the introduction of the agrochemical:

175.2 °C to 129.6 °C and 110.0 °C → **plasticizing effect**

Formation of two separate melting points

at 110 °C

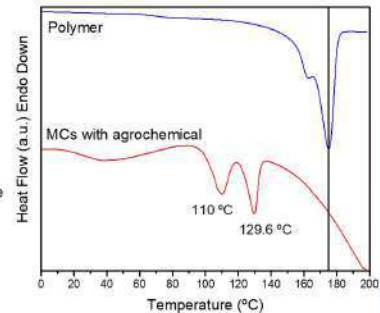
Polymer crystalline structure richer in agrochemical

Last portion of the MC to solidify

at 129.6 °C

Polymer crystalline structure poorer in agrochemical

First portion of the MC to solidify



XRD

Shift of the polymer peaks to the right

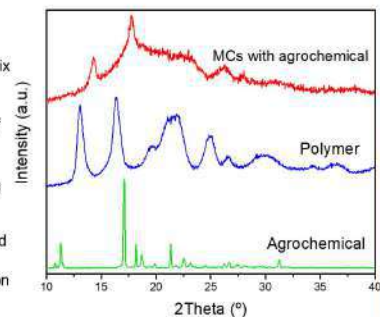
Decrease in the **interplanar spacing** of the polymeric matrix

Decrease of the **polymer free volume** in the presence of the agrochemical

Compression of the polymeric lattice by the encapsulated material

Agrochemical in the **amorphous state** when encapsulated

Higher efficiency in application



Conclusions

- ✓ Successful production of loose and spherical MCs with a matrix-type structure, containing an agrochemical and a biodegradable polymeric matrix;
- ✓ Median size below 10 mm with a narrow standard deviation, high loadings and high encapsulation efficiencies achieved;
- ✓ Structural changes in the matrix with the introduction of the agrochemical;
- ✓ Solvent evaporation emerges as a possible microencapsulation process to produce biodegradable particles in line with recent EU legislation;

Acknowledgments: The authors work within the TECHNOLOGY PLATFORM OF MICROENCAPSULATION AND IMMOBILIZATION, TPMI (ulisboa.pt) and gratefully acknowledge Fundação para a Ciência e a Tecnologia (FCT) through the support of CERENA (FCT-UIDB/04028/2025), the grant 2024.00327.BDANA (LPM) and the contract 2023.15700.TENURE.037/CP00055/CT00014 (A. A.), using national funds. The authors also acknowledge the financial support by Ascenza SA, as well as Dr. Edgar Felizardo from Instituto de Plasmas e Fusão Nuclear (IST-ID) for helping with the training and giving access to the XRD equipment used in this work.

From Pruning to Harvest: Evaluating Proxy Consistency in Smallholder Semi-Arid Vineyards

PhD Exchange (INPE/Brazil)
 Heithor Queiroz (heithorqueiroz@gmail.com)
 Supervisor: Maria Paula Mendes

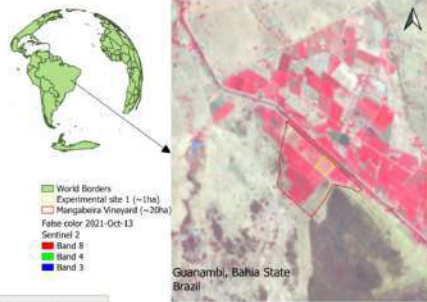
Overhead trellising (*latada/pergola*)* versus Vertical trellising



- *Protection against weather risk:
- low rainfall (25-50 cm annually)
 - high temperature
 - low moisture
 - high evapotranspiration
 - land shaped by erosion



Novelty: fragmentation, small plot sizes (<10ha), and a lack of in-situ calibration data

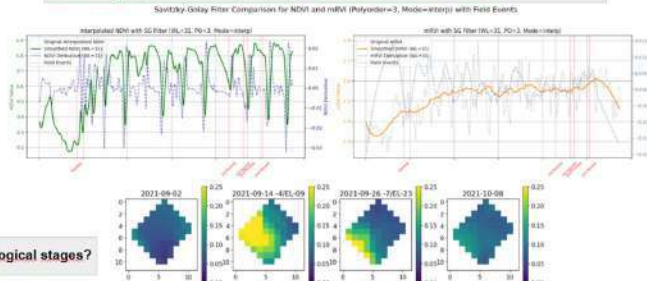


2 irrigated grapevine species: Guanambi, BA (cultivar Isabel Precoce) and Petrolina, PE (cultivar ARRA 15 Sweeties™).



- *2,5 cycles per year
- *different amplitude between species

We are denoising Sentinel-1 (radar) and Sentinel-2 (optical) data through cloud filtering, smoothing, and interpolation, ensuring no critical information is lost.



Which proxy is more suitable to the ground truth field-observed phenological stages?



Preliminary data on long bone histology of *Eousdryosaurus* sp. (Ornithopoda: Dryosauridae) from the Upper Jurassic of Portugal.

Programa Doutoral em Energia e Recursos da Terra

Bruno Camilo (bruno.camilo.da.silva@tecnico.ulisboa.pt)

Supervisor: Ricardo Araújo

Introduction

Paleohistology has been used to infer various aspects of fossil vertebrate biology, such as growth strategies, growth curves, skeletochronology, and ontogeny. Here we present preliminary results on the palaeobiology of three specimens of *Eousdryosaurus* sp., a small, bipedal, herbivorous ornithopod dinosaur exclusive to the Upper Jurassic fossil record of Portugal (Escaso et al 2014; Rotatori et al., 2020), representing two distinct morphotypes based on the size of the femurs and tibiae. The null hypothesis postulated that the individual represented by the larger femur and tibia would represent a skeletally mature individual, and the smaller specimens would represent juvenile ontogenetic stages. Histology demonstrated different growth strategies between the two morphotypes, with ontogenetic development differing between them, suggesting high intraspecific variability.

Geographic and Geological Setting

The specimens were collected from the coastal cliffs of the central sector of the Lusitanian Basin (Portugal), in the municipalities of Peniche and Lourinhã, respectively in the Bombarral Formation (Kimmeridgian) and Praia da Amoreira-Porto Novo Formation (Upper Kimmeridgian). Both formations are associated with the continentalization of the Lusitanian Basin during the Upper Jurassic period and marked by the establishment of transitional environments.

Sampled material

SHN.(JJS).007- an isolated femur; SHN.(JJS).170 (Holotype of *Eousdryosaurus nanohallucis*- Femur and Tibia; SHN.(JJS). Femur and Tibia (larger morphotype).

Discussion and conclusions

The histological analysis of three dryosaurids from the Upper Jurassic of Portugal, *Eousdryosaurus nanohallucis* (SHN.(JJS).170), a specimen attributed to *Eousdryosaurus* sp. (SHN.(JJS).007) and a larger specimen aff. *Eousdryosaurus* sp. (SHN.004), has revealed different growth trajectories between the smaller specimens and the larger morph. The comparable tibia from the holotype and the large morph have demonstrated different patterns of vascularity, vascular orientation, and cyclicity. Despite showing more Growth Marks (GM), the overall bone tissue of the larger specimen reveals more juvenile bone and a faster growth, which may be assumed for a larger animal, and less variation on the types of bone deposited and vascularity throughout the entire cortex. The femur of this specimen shows the same pattern of bone deposition, vascular organisation and a number of GM (between 8 and 10) as the tibia; both with a marked slowdown of apposition rate after the 5th cycle (attained sexual maturity). In relation to SHN.(JJS).007, the femur shows a more or less similar growth trajectory to the femur of the holotype. However, despite being slightly larger, it shows it to have been younger, with 4 GM. The tibia from the holotype shows a better record than the femur with at least 6 LAG's and alternating types of bone with fast and slower growth rates.

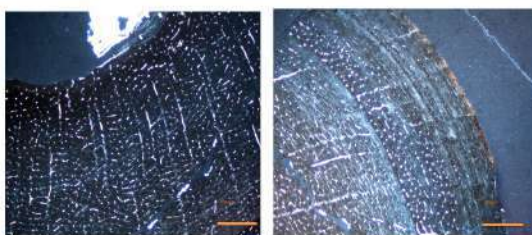


Figure 1- Thin section of *Eousdryosaurus* tibia (holotype)
A- inner cortex with fibrolamellar bone, with alternating radial and circumferential orientation. B- cyclicity between woven bone (innermost cortex) with parallel fibered bone and the decrease in vascularity towards the outermost cortex. Cross-polarized with lambda filter.

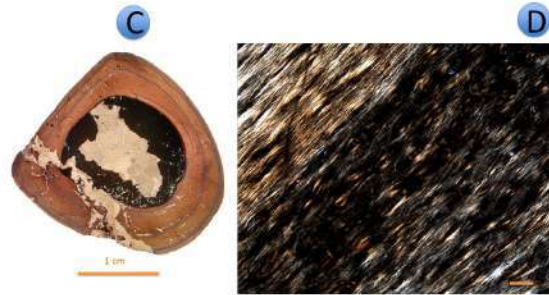


Figure 2 - SHN.(JJS).007.

A- Whole transverse section of the dryosaurid SHN.(JJS).007 with LAG's/GM. B- vascular and fibrillar organization in the middle part of the cortex, showing highly vascularized fibrolamellar bone. Cross-polarized with lambda filter



Figure 3 - SHN.(JJS).004.

E- Core drill of the femur, showing growth marks endosteal to the outer most cortex. Transmitted light. F- Section of the tibia showing variability and alternation of bone tissues from the fibrolamellar complex, with radial and longitudinal (reticular) orientation.

They share the same similarities with regard to other closely related dryosaurids (and other small basal iguanodontians), such as *Dryosaurus* and *Dysalotosaurus* (Horner et al, 2009; Hubner, 2012), namely a moderate to fast sustainable growth, a lack of an External Fundamental System, and a low degree of secondary remodelling. They differ, however, in the presence of Lines of Arrested Growth (LAG) when compared with the same ontogenetic class sizes. It seems that Portuguese dryosaurids developed LAG's very early, maybe in the juvenile ontogenetic stage. At least the holotype of *Eousdryosaurus* and SHN.004 seem to have reached sexual maturity as late juvenile or as young subadult, in contrast with the delayed onset of sexual maturity in *Dryosaurus* and *Dysalotosaurus* (reproductively active around 10 years of age). With regard to SHN.004, and despite being taxonomically indistinguishable from smaller specimens is here regarded as possibly representing a different population, suggesting a disparity of plasticity and/or intraspecific variability within *Eousdryosaurus*.

References:

- Escaso et al. (2014), A new dryosaurid ornithopoda (Dinosauria, Ornithischia) from the late Jurassic of Portugal. *Journal of Vertebrate Paleontology*, 34(5), 1102-1112
- Horner et al. (2009), Comparative long bone histology and growth of the "hybridophorid" dinosaurs *Ondromenus makelai*, *Dryosaurus altus*, and *Tenontosaurus silletti* (Ornithischia: Euornithopoda). *Journal of Vertebrate Paleontology*, 29(3), 734-747
- Hubner, T. (2012), Bone histology in *Dysalotosaurus fetznerbecki* (Ornithischia: Iguanodontia) - variation, growth, and implications. *PLoS One*, 7(1), e29558
- Rotatori et al. (2020), New information on ornithopod dinosaurs from the Late Jurassic of Portugal. *Acta Paleontologica Polonica* 65 (1): 35-57.

Scars from a Fire: Assessing Vulnerability and Performance

PhD in Earth Resources

Roberta Lobarinhas (robertalobarinhas@tecnico.ulisboa.pt)

Supervisors: Amélia Dionísio, Gustavo Paneiro

Introduction

Fire exposure can significantly modify the hydric behaviour of natural stones, with direct implications for post-fire durability and long-term damage susceptibility (Fig.1). While post-fire assessments often prioritise mechanical integrity, thermally induced changes in water transport and retention play a critical role in subsequent decay processes. This study introduces a new methodological perspective by analysing hydric susceptibility as a time-dependent process (Fig. 2), considering not only the rate of water absorption, but also the duration of moisture retention after thermal exposure, since prolonged water presence increases the risk of water-related deterioration processes such as salt crystallisation and biocolonization.



FIGURE 1: São Domingos Church: after 1959 fire (a), and at 2026 (b).

Results and Discussions

The study analysed a broad set of carbonate stones, including 8 limestones, 3 marbles, a breccia and a travertine, with distinct grain sizes and pore networks.

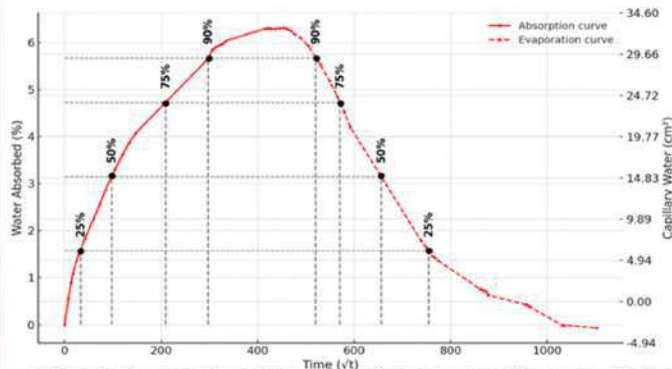


FIGURE 2: Example of a capillary absorption and evaporation curves. Dashed lines indicate the time points at which 25%, 50%, 75%, and 90% of total water absorption (WA%) were reached.

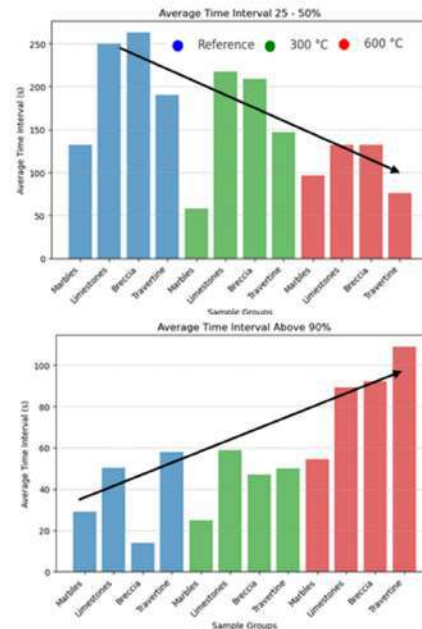


FIGURE 4: Average time intervals (s) for the different lithologies within defined water absorption percentage (WA%) ranges (25–50% and above 90%) at the Reference conditions and heated at 300 °C and 600 °C.

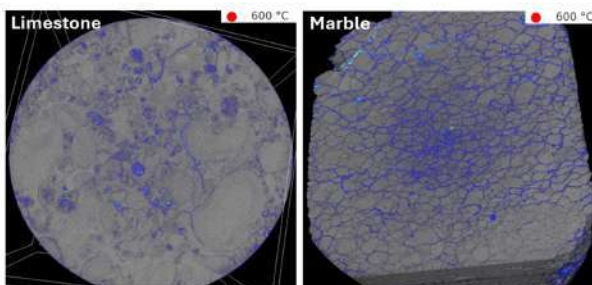


FIGURE 3: Nano CT of Limestone and Marble samples heated at 600 °C.

All stones were subjected to controlled thermal exposure (300 °C and 600 °C), allowing direct comparison of hydric behaviour before and after heating. Thermal exposure induced systematic microstructural changes, in limestones (Fig. 3), the original pore network was progressively altered by microcracking, pore widening, and increased connectivity. These structural modifications resulted in enhanced water uptake but, more importantly, in significant changes in moisture retention behaviour. In contrast, marbles exhibited higher microcracking processes, which led to faster water absorption but also release, leading to shorter retention times. These differences became especially evident when hydric susceptibility was analysed as a time-dependent process (Fig. 4). While capillary absorption coefficients increased for most lithologies after heating, they did not reliably reflect the observed vulnerability.

Several limestones showed moderate capillarity but remained saturated for prolonged periods, whereas marbles, despite rapid absorption, dried significantly faster.

Conclusions

This demonstrates that retention time is more sensitive to thermally induced microstructural damage than capillary coefficients alone. By linking petrographic features to hydric dynamics, the results show that the evolution of the pore network in limestones strongly favours prolonged moisture residence, increasing susceptibility to water-related decay mechanisms such as salt crystallization and biocolonization. These findings confirm that post-fire hydric vulnerability is controlled not only by how quickly water enters the stone, but by how long it remains within its structure.

Acknowledgments

This work was financially supported by UID/04028 of the CERENA—Research Center for Natural Resources and Environment—CERENA—funded by Fundação para a Ciência e a Tecnologia, I.P./ MECI through the national funds. Doctoral grant UI/BD/152298/2021.

Fire as a risk and a resource to the pre-historic artists: Through the lens of Geosciences

PhD in Energy and Earth Resources
 João Senra (joao.senra@tecnico.ulisboa.pt)
 Supervisors: Amélia Dionísio / Gustavo Paneiro / Thierry Aubry

Introduction

Rock art, human-made artwork created through the addition of pigments or the removal of bedrock, is among the earliest forms of human artistic expression. However, the preservation of these cultural assets is increasingly threatened by environmental agents, particularly those intensified by climate change (Bertolin 2019). Most research on the impact of climate change in rock heritage focuses on environmental agents derived from events such as sea-level rises, storm events and glacial. Meanwhile, research on the threat of fire as an environmental agent in rock heritage – and rock art in particular – remains in its early stages, particularly when it comes to the development of experimental methods to study such an impact (Lobarinhas et al. 2024).

Objectives

O1 – Better insight on high temperature deterioration of Rock Engravings

O2 – Design In-Situ methodology to analyze fire deterioration

O3 – Evaluate long-term performance of phyllites after a fire event

Study Area

This PhD project appears as an opportunity to increase our knowledge about the effects of high temperatures, that occur during wildfires, on rock-art panels and portable rock art. This project is evaluating the impact of wildfires on the engraved phyllites of the Côa Valley Archaeological Park (CVAP) (Fig.1). CVAP is located in the northeastern region of Portugal, currently listed as a World Heritage Site by UNESCO and widely considered one of the most important Open-Air Rock Art Sites (OARS) of the Paleolithic era (Luís 2003).

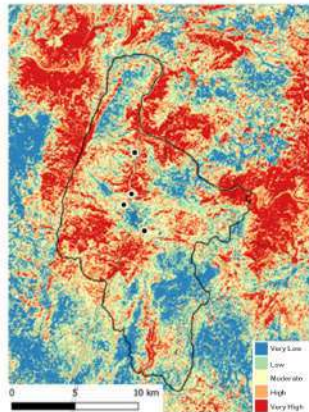


Fig.1 Côa Valley Special Protection Zone (CVAP) and the four major study areas, within the context of Fire Risk Assessment of the region

Results

Data from the non-destructive standardized testing shows that the phyllites present a color change with increasing temperature from gray to orange (Fig.3), while properties such as water capillary absorption and open porosity tend to present increases (Fig.4 & 5) and P-wave propagation velocity presents decreases (Fig.6). Some properties are affected by sample characteristics:

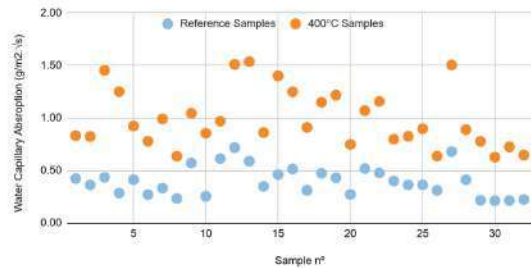


Fig.4 Water capillary absorption(g/m2.vs) in phyllites at 25°C and 400°C.

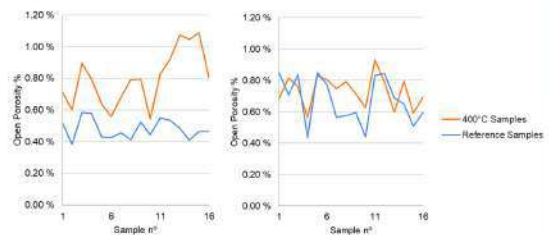


Fig.5 Open porosity (%) in phyllites at 25°C and 400°C, in samples exposed to freeze-thaw weathering cycles (left) and reference samples (right).

Open porosity values in samples exposed to high-temperatures are dependent on sample weathering (Fig.5), while P-wave propagation velocity increases are highly dependent on phyllite foliation direction (Fig.6).

Materials and Methods



The sampling campaign consisted of georeferenced phyllite samples collected from CVAP, near rock art panels in four major study areas (Fig.2), along with phyllite samples from a nearby quarry.

Fig.2 Fire decay patterns observed in CVAP phyllite open-air rock sites, near engraved artworks in Canada do Inferno, one of the locations studied.

These samples then went through standardized non-destructive testing of physical and mechanical properties, before and after being exposed to high temperatures (Fig.3). The high temperature tests were performed in an electrical oven with target temperatures of 200°C, 400°C and 600°C, and heating rate of 12°C/min and an exposition time of 1h, which are common values for experimental tests in rock materials (Tomás et al. 2025).

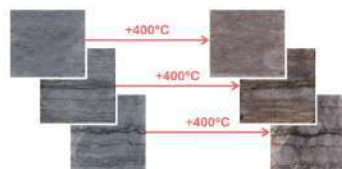


Fig.3 Quarry phyllite samples before and after exposure to 400°C (12°C/min heating rate and exposure time of 1h).

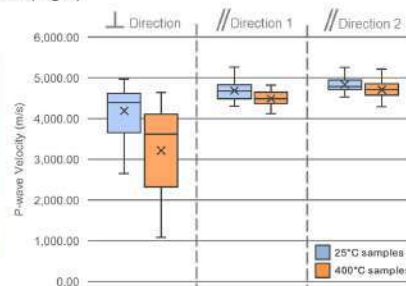


Fig.6 P-wave propagation velocity boxplot comparing reference phyllite samples (gray) and samples exposed to 400 °C (red), measured perpendicularly (left), and parallel (center, right) to the direction of sediment deposition.

Acknowledgements:

This work was financially supported by UIDB4028 of the CERENA—Research Center for Natural Resources and Environment—funded by Fundação para a Ciência e a Tecnologia, I.P./MEC through the national funds Doctoral grant 2023.04109.BDANA

References:

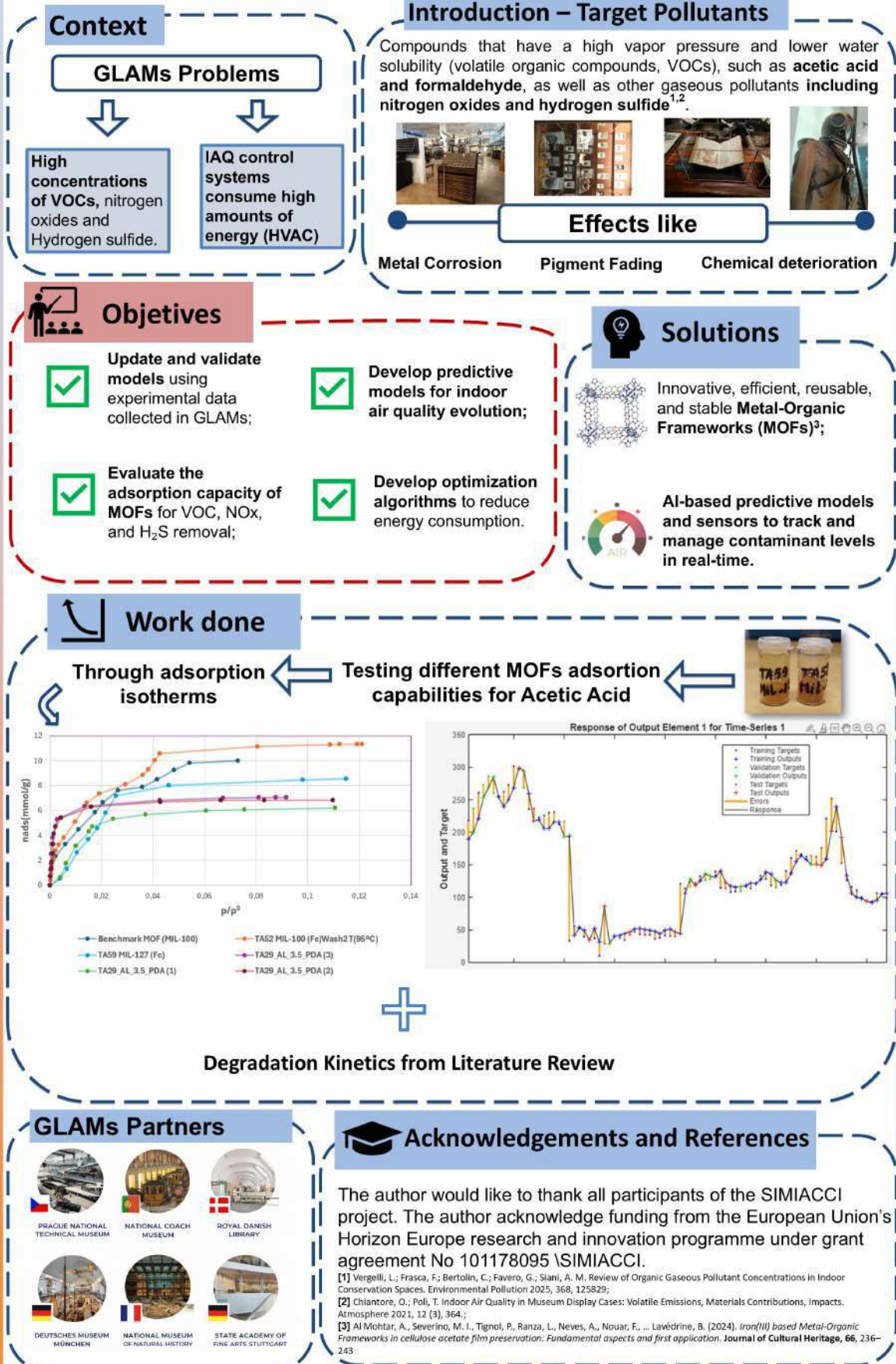
Bertolin C (2019) Preservation of Cultural Heritage and Resources Threatened by Climate Change. *Geosciences* 9:250.
 Luís L (2003) Sauvageado, conservação e valorização do património de la Vale do Côa (Portugal), in *Vestigios arqueológicos em meio extremo*. Paris: Institut National du Patrimoine. Monum, Editions du Patrimoine: 110-119.
 Lourenço R, Dantas A, Paneiro G (2024) High Temperature Effects on Global Heritage Sites Resources: A Systematic Review. *Heritage* 7:6310-6342.
 Tomás R, Beavente D, Martínez-Ibañez V, & Camilo ME (2025) How do high temperatures affect rock properties? A comprehensive review of experimental thermal effects and underlying mechanisms. *Engineering Geology* 357:108323.

Intelligent Management of Indoor Air Quality in GLAMs

SIMIACCI Project – PhD in Chemical Engineering

Miguel Vitoriano Teixeira (miguel.vitoriano.teixeira@tecnico.ulisboa.pt)

Supervisors: Dra. Abeer Mohtar and Prof. Moisés Pinto



Green Hydrogen Production in Cape Verde from Renewable Energy Sources

PhD in Chemical Engineering

Tomás Felismino Furtado Tavares (tomas.tavares@docente.unicv.edu.cv)
Supervisors: Prof. Rui Manuel Gouveia Filipe, Prof. Carla Isabel Costa Pinheiro

Abstract

This study evaluates a hybrid solar–wind system for green hydrogen production in Cape Verde. HOMER Pro software is used to obtain optimized hybrid configurations for energy production based on hourly solar, wind, and load profiles. The aim is to assess the techno-economic feasibility of green hydrogen production units to complement the existing solutions based on fossil fuels in Cape Verde Islands.

Introduction

- Global dependence on fossil fuels increases CO₂ emissions and climate change.
- Green hydrogen produced from renewable energy sources is a clean energy solution.
- Main applications: industry, mobility, and energy storage;
- High potential in countries with abundant renewable resources, such as Cape Verde Islands.

Motivation: energy context of Cape Verde

- 80 % dependence on imported fossil fuels (see Fig. 1).
- 20 – 25 % renewable energy integration in the national electrical grid and the goal to increase to 100 %.
- High solar and wind potential, enabling green hydrogen production.



Figure 1: Fuel sales by product in Cape Verde (m³), 2017–2022. Source: Cape Verde National Statistics Institute.

Objective

- Review national energy policies and regulatory frameworks for the deployment of green hydrogen.
- To evaluate the technical and economic feasibility of green hydrogen production in Cabo Verde using hybrid solar–wind energy systems.
- To model and optimize renewable-powered hydrogen production systems for island energy contexts.
- To assess the potential contribution of green hydrogen to the energy transition and security.

References

- Behabtu, H. A., Messagie, M., Coosemans, T., Berecibar, M., Fante, K. A., Kebede, A. A., & Van Mierlo, J. (2020). A review of energy storage technologies' application potentials in renewable energy sources grid integration. *Sustainability (Switzerland)*, 12(24), 1–20. <https://doi.org/10.3390/su122410511>
- Beidaghi, M., & Gogotsi, Y. (2014). Capacitive energy storage in micro-scale devices: Recent advances in design and fabrication of micro-supercapacitors. In *Energy and Environmental Science* (Vol. 7, Issue 3, pp. 867–884). <https://doi.org/10.1039/c3ee43526a>

Methods and Procedures

- **The system architecture:** consists of an off-grid hybrid system with a solar-wind setup, battery storage and water electrolysis.
- **Resource and load data:** the daily solar radiation, clearness index, Wind Speed and temperature data from NASA databases for Santiago Island, together with representative load profiles and component cost, were used as inputs.
- **Optimization criteria:** the system was optimized by minimizing the net present cost, using the levelized cost of energy and renewable energy fraction.

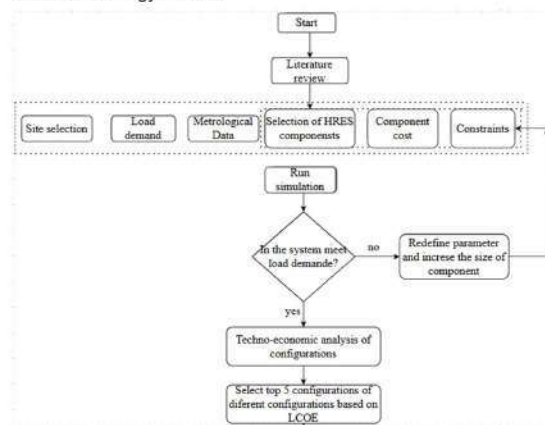


Figure 2: Flowchart of hybrid system for hydrogen production. Adapted from P. Kumar et al (2025).

Expected results

- The optimized hybrid solar–wind system on Santiago Island is expected to produce approximately 3.4 kt/year of green hydrogen, thereby demonstrating the technical feasibility of such systems in island energy contexts.
- The estimated levelised cost of energy (LCOE) is approximately 0.10 € /kWh.
- The estimated levelized cost of hydrogen (4.5–8.13 €/kg) there is strong potential for Cabo Verde to use hydrogen to support the energy transition and ensure energy security.

Conclusion

- This study demonstrates the technical and economic potential of green hydrogen production in Cabo Verde using hybrid renewable energy systems.
- The proposed modelling framework enables robust assessment of hydrogen deployment scenarios in island energy systems with high renewable resources.
- The aim of this study is to support evidence-based energy policy and contribute to a sustainable energy transition in Cape Verde.

Acknowledgements

This work was funded by the Fundação para a Ciência e a Tecnologia (UID/00100/2025, UID/PRR/100/2025, FCT-UIDB/04028/2025, FCT-UIDP/04028/2025, PRT/BD/154847/2023) and hosted by CERENA.

Technoeconomic impact of impurities on CO₂ injection in EOR and Geo-storage

Shahmir Noshervani (shahmir.noshervani@tecnico.ulisboa.pt) - PhD Program in Chemical Engineering



Motivation and Objectives

- Carbon Capture, Utilization & Storage (CCUS) is key to meeting IPCC 2050 emission goals → **Capturing and Storing 5000-10000 Mt CO₂/yr.**
- One way that may enhance the feasibility of CCUS deployment is by reducing costs → **Decrease the purity level of the CO₂ stream.**
- Objective**
Develop a **technoeconomic numerical tool** to evaluate CO₂-EOR and CO₂-geostorage systems under varying CO₂ purities, quantifying impacts across the entire value chain: **capture** → **transport** → **geo-storage**.



Data and Methods

- Scope:** Integrated model covering (Fig.1):
 - Power and Process Plants (with Capture processing units) – 11 industries
 - Pipeline transport (gas/liquid/Onshore/Offshore)
 - Reservoir (EOR/ Geo-storage)
- Purity control:** CO₂ purity decreased via a bypass valve and bypass compression system (Fig. 1). – 8 industries
- Economic indicator:** Levelized Cost (LC)
LCH = LCP + LCT + LCS + LCU
H = whole chain, P: capture, T: transport, S: storage, U: utilization (EOR)
- Simulation:** 3-D numerical flow model (tNavigator) for two injection cases (Fig.2):
 - Case 1 – 100% Pure CO₂
 - Case 2 – 80% Pure CO₂ (remaining 11% N₂, 1.6% H₂S, 2.3% O₂, 4.2% H₂O, 0.3% SO₂, 0.3% CO and 0.4% NO₂)
 Injection: ~1 Mt/yr for 25 yrs + 100 yrs plume observation.

Distance from emission source to storage site: 500 km

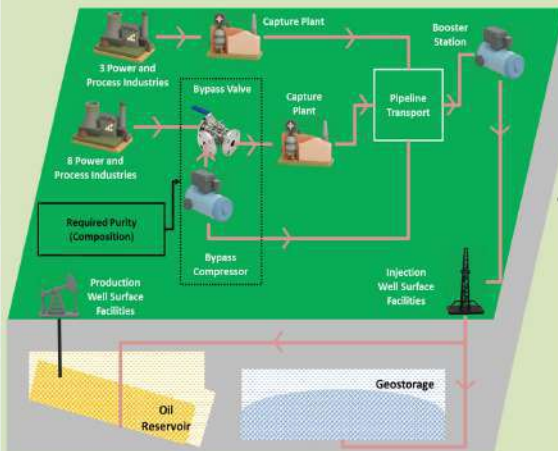


Figure 1. Integrated CCUS value chain in this tool

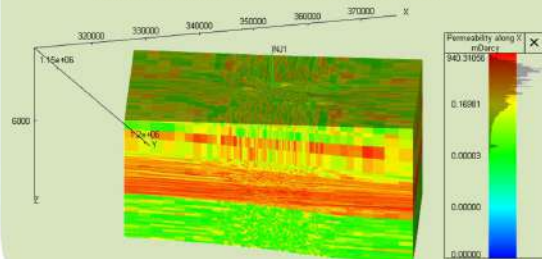


Figure 2: Permeability distribution of Illinois Decatur Project reservoir



Results

- Plant stage:** 20% purity reduction → CAPEX ↓ \$ 0.16 bill., OPEX ↓ \$ 0.09 bill./yr
- Pipeline transport:** 20% purity reduction → CAPEX ↑ \$0.84 bill., OPEX ↑ \$14 mill./yr, LCT ↑ \$2-2.4/t.
- Reservoir performance:** Impurities → larger plume spread, altering storage dynamics (Fig. 3)
- Geo-storage economics:** CAPEX ↑ \$7.6-7.8 bill., OPEX ↑ \$113-114 mill./yr
- Levelized Costs:** LCP ↓ \$18/t, LCT ↑ \$2/t, LCS ↑ \$0.17/t. (Fig.4)
- Overall value chain:** LCH ↓ \$14/t (↓ 9%) from Case 1 → Case 2, indicating impurities can reduce total chain cost. (Fig.5)

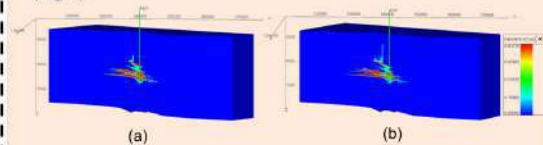


Figure 3. Saturation of gas, at the end of 125 years, in: (a) Case 1 (b) Case 2

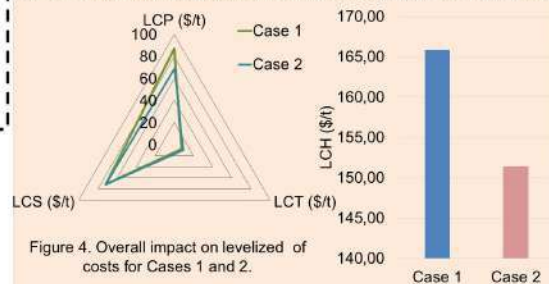


Figure 4. Overall impact on levelized of costs for Cases 1 and 2.

Figure 5. Overall economic performance of value chain for Cases 1 and 2.



Conclusion and Future Work

- Reduction in purity, makes the value chain more feasible by 8.7%.
- The assumption in the technoeconomic tool is the use of trunk pipeline, however in the future work it should be considered. Moreover, research is required on the fluid dynamics in the pipeline, in case of impure CO₂ transport.
- Finally, study the geochemical impact of impure CO₂ stream as it is highly geological specific as it may increase or decrease injection depending on the rock matrix and injected fluid composition.

References

[1] IPCC, "Climate Change 2014: Synthesis Report. Contribution of Working Groups I, II and III to the Fifth Assessment Report of the Intergovernmental Panel on Climate Change," 2014

Acknowledgements

The author acknowledge the support of the CERENA (strategic project FCT-UIDB/04028/2020), FCT for the strategic project UI/BD/152299/2021.

Supervisors

Professor Moisés Pinto, Department of Chemical Engineering, Instituto Superior Técnico
Professor Leonardo Azevedo, Department of Mining and Energy Resources Engineering, Instituto Superior Técnico

CO₂ valorisation with Earth abundant metals: From bench to pilot

PhD in Chemistry in Faculty of Sciences of the University of Lisbon
Rafaela Tenera Marques (rfmarques@fc.ul.pt)
Supervisors: Sara Realista, Rui Galhano dos Santos, Paulo Nuno Martinho

Introduction

- CO₂ plays a crucial role in the carbon cycle, which keeps the Earth's temperature stable.
- The increased in CO₂ concentration has unbalancing the carbon cycle, affecting our planet's energy balance.
- The **carbon dioxide reduction reaction (CO₂RR)** to **carbon monoxide, formic acid, methanol, methane**, among others, is one of the most interesting pathways for carbon dioxide utilisation.
- The **photoconversion** of CO₂ can be made in homogeneous media and requires three components: the **catalyst (CAT)**, which in the active form, converts CO₂, the **sacrificial donor (SD)**, donates electrons and is consumed and the **photosensitizer (PS)**, absorbs light and mediates the electronic transfer between the catalyst and the sacrificial donor.
- Different components can be added to the catalytic system to improve the catalytic performance, such as, ionic liquids and a reversible quencher, that mediates the electron transfer between the PS and SD.

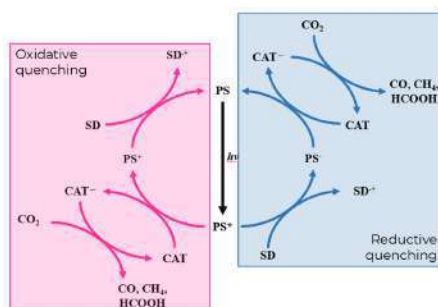
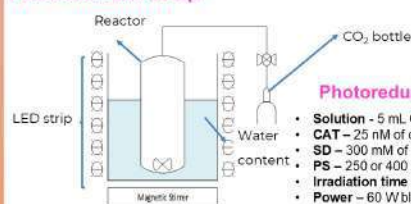


Fig. 1. Photocatalytic mechanism of carbon dioxide conversion. The mechanism could have two pathways the oxidative quenching (pink) or the reductive quenching (blue).

Photoreduction experiments at smaller scale

Photoreduction setup



- Photoreduction conditions**
- Solution - 5 mL CH₃CN/H₂O (4:1)
 - CAT - 25 nM of cryptate C_{CoCoBr} or C_{CoZnBr}
 - SD - 300 mM of Triethanolamine
 - PS - 250 or 400 mM of [Ru(phen)₃](PF₆)₂
 - Irradiation time - 30 h
 - Power - 60 W blue LED lights (400 nm).

Fig. 3. Setup and conditions used in the photocatalytic CO₂ experiments at smaller scale.

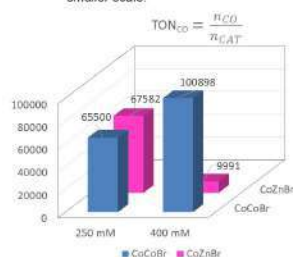


Fig. 4. TON_{CO} values for different cryptates C_{CoCoBr} or C_{CoZnBr}.

The TON was used to assess catalyst efficiency, and the TOF was used to measure catalyst robustness.

Comparing both 0.4 mM and 0.25 mM experiments, several conclusions can be drawn:

- C_{CoCoBr} - decreasing PS by 42.5% led to a 45% reduction in TON_{CO}
- C_{CoZnBr} - decreasing PS by 42.5% led to a 165% increase in TON_{CO}
- TON_{CO} of C_{CoZnBr} at 0.25 mM is 21% lower than that of C_{CoCoBr} at 0.4 mM

Catalysts synthesis

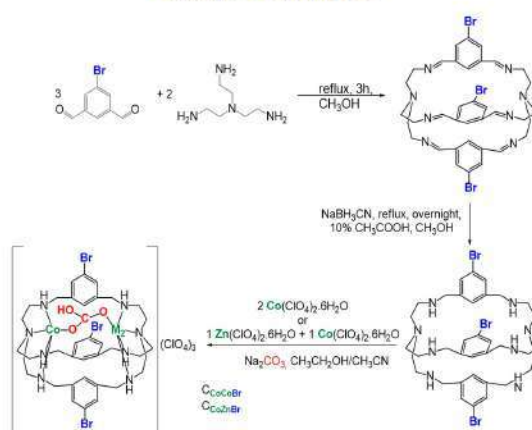
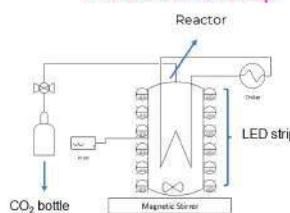


Fig. 2. Synthesis of C_{CoCoBr} or C_{CoZnBr}, that will be used for photocatalysis.

Photoreduction experiments at larger scale

Photoreduction setup



Photoreduction conditions

- Solution - 500 mL CH₃CN/H₂O (4:1)
- CAT - 25 nM of cryptate C_{CoCoBr}
- SD - 300 mM of Triethanolamine
- PS - 400 mM of [Ru(phen)₃](PF₆)₂
- Irradiation time - several days
- Power - 90 W blue LED lights (400 nm).

Fig. 5. Setup and conditions used in the photocatalytic CO₂ experiments at larger scale.

Cycle number	Days of the maximum TON obtained	Maximum TON _{CO} obtained	Maximum TON _{CH₄} obtained
1	5	1005	110
2	7	649	251
3	8	1279	193
4	9	2105	170
5	8	2061	68
6	7	2675	0

Tab. 1. TON_{CO} and TON_{CH₄} values obtained for C_{CoCoBr} in the photocatalytic CO₂ experiments at larger scale.

Conclusions and future work

- All of the experiments at smaller scale presented CO selectivity values above 90%.
- C_{CoCoBr} - presented the better results with 400 mM of PS.
- C_{CoZnBr} - with the decrease of PS to 250 mM of PS the results improved.
- For the experiments at larger scale, C_{CoCoBr} was used as CAT, and the volume was increased 100 times.
- At larger scale it is possible reused the solution and so far as much the solution is used better TON_{CO} are obtained but lower amounts of CH₄ are detected.
- More tests at larger scale are needed to understand this results and more cycles are being tested.

Acknowledgments

We are grateful to Fundação da Ciência e a Tecnologia, FCT, for Project PTDC/QUI-QIN/0252/2021.

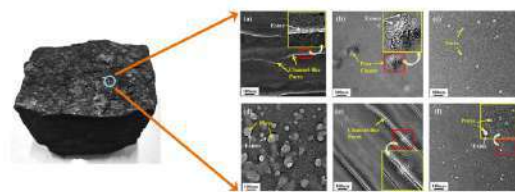
Exploring the pore structure of coal at the microscale

Xiaodong Guo (xiaodong.guo@tecnico.ulisboa.pt)

Supervisor: Yixin Zhao, Helga Jordão

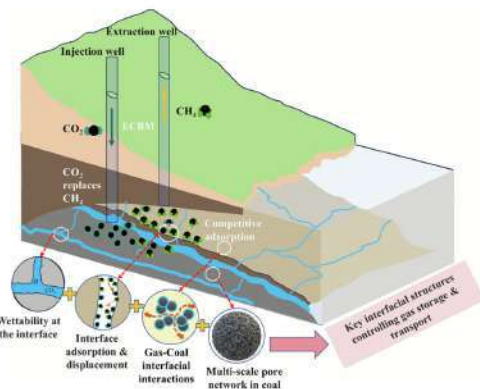
The complex pores of coal

The pore structure of coal exhibits significant complexity. From a microscopic perspective, it is characterized by the development of multi-scale and multi shaped pore systems, such as channel like pores, pore clusters, and dispersed pores. The development characteristics and spatial distribution of these pores profoundly affect the adsorption behavior and transport performance of coal towards gases.



The microscopic pore structure of coal.

In the macro engineering practice, the coalbed methane development technology ECBM relies on the multi-scale pore network of coal to achieve the process of CO₂ injection to replace CH₄. CO₂ occupies the adsorption sites on the surface of coal pores through competitive adsorption, and completes gas storage and transport through the pore network, thereby promoting the desorption and production of CH₄. The heterogeneity of micro pore structure directly determines the gas displacement efficiency and reservoir transformation effect in macro engineering, providing key scientific basis for optimizing coalbed methane development technology and improving resource recovery.

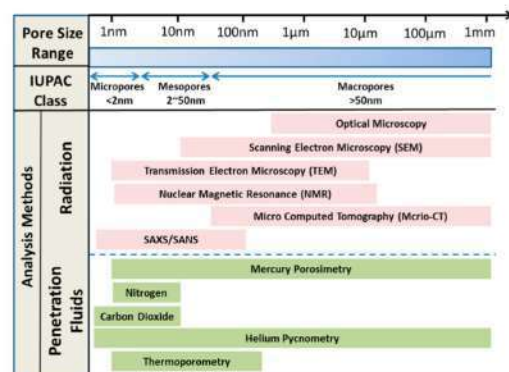


Multi-scale schematic of CO₂-ECBM in coal reservoir.

The detection for micropore structure

The detection methods for coal micro pore structure exhibit diverse characteristics. Different technologies play a unique role in pore characterization due to differences in principles and applicable scales. On the one hand, radiation methods include scanning electron microscopy, transmission electron microscopy, nuclear magnetic resonance, computed tomography, and small angle scattering techniques.

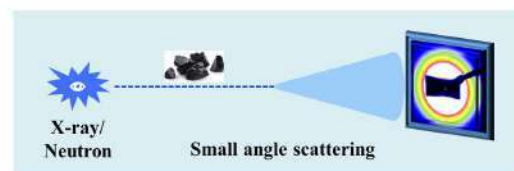
On the other hand, fluid permeation methods include mercury porosity, gas adsorption, helium pycnometry, thermoporometry, etc. These methods together constitute a multidimensional detection system for coal pore structure, providing technical support for accurate characterization of pores at different scales.



The detection range of different techniques.

Small angle scattering technology

Small angle scattering techniques (SAXS and SANS) are important branches of radiation-based methods. This technology refers to the scattering phenomenon generated by the sample within 5°. With non-destructive, high sensitivity, and the ability to detect nanoscale pores, it has demonstrated unique value in the study of coal micro pore structure. The scattering signals generated by the interaction between X-rays or neutron beams and coal samples can be used to analyze the size, shape, and distribution characteristics of pores. This provides a key means for a deeper understanding of the nanoscale structure of coal pores.



The principle of small-angle scattering technology.

References

- Elsevier, 2023, ISBN: 978-0-323-95297-2.
- Adv. Colloid Interface Sci., 2026, 349: 103769.
- Gas Science and Engineering, 2025, 134: 205540.
- Fuel, 2023, 345: 128261.
- Energy & Fuels, 2014, 28(6), 3704–3711.

Multidimensional stochastic mine planning and design for sustainable mining CRITERIA Project

Jakub Franciszek Skiba^{1,2} (jakub.skiba@tecnico.ulisboa.pt)

Leonardo Azevedo^{1,2}, Ana Margarida de Sousa^{1,2}, Marc Bascompta³

¹DER, Instituto Superior Técnico (IST), University of Lisbon, Portugal ²CERENA, Portugal ³Universitat Politècnica de Catalunya, Spain

Objectives

The objective of the project is the integration of uncertain socio-environmental variables into the stochastic mine planning and optimization framework.

- Selection of an **appropriate domain of study and variables** to be addressed
- Inclusion of classical **economic metrics** such as Net Present Value (NPV) and Cut-off Grade (COG)
- Integration of **environmental variables**, such as energy use, waste generation, and air pollution
- Integration of **socio-economic** considerations, such as population displacement
- Creation of an applicable **stochastic algorithm** suitable for use in the industry

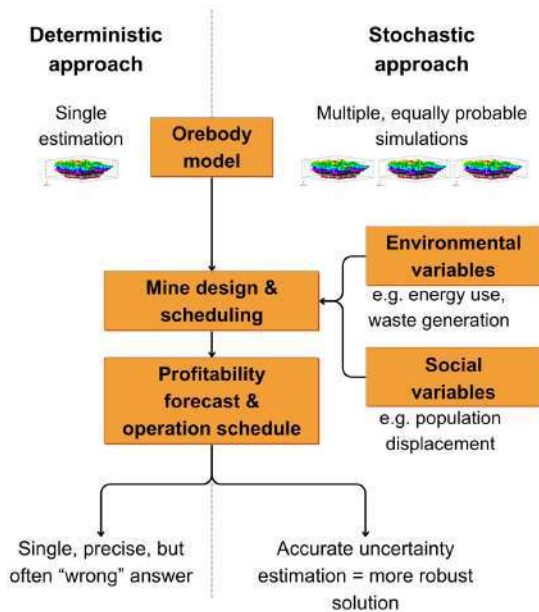


Figure 1. Comparison of the deterministic and stochastic approaches with novel contributions

Such methods were successfully used to optimize economic parameters of mining operations, such as net present value (NPV) and cut-off grade (COG) [1,2], resulting in more robust operation schedules and more profitable mine designs. Recent works also highlight the potential of stochastic mine planning methods in addressing socio-environmental and governance (ESG) issues [1,3]. However, this area remains underdeveloped, which this project aims to expand.

Acknowledgments

This project has received funding from the European Union's Horizon Europe Marie Skłodowska-Curie Actions Doctoral Networks under Grant Agreement No 101169238

Methodology

The project commences with a **systematic literature review (SLR)** to identify the most prominent stochastic mine planning methodologies and potential **research gaps**, as well as to narrow down the **domain of the project**. This stage is followed by the development of a comprehensive **algorithm** that aims to incorporate ESG concerns into the objective function. This will be done in cooperation with the counterparts at UPC. The algorithm in question is then to be applied in a **practical case study** developed with the industrial partner, Minerali Industriali. The outline of the methodology is provided in (Fig. 2).

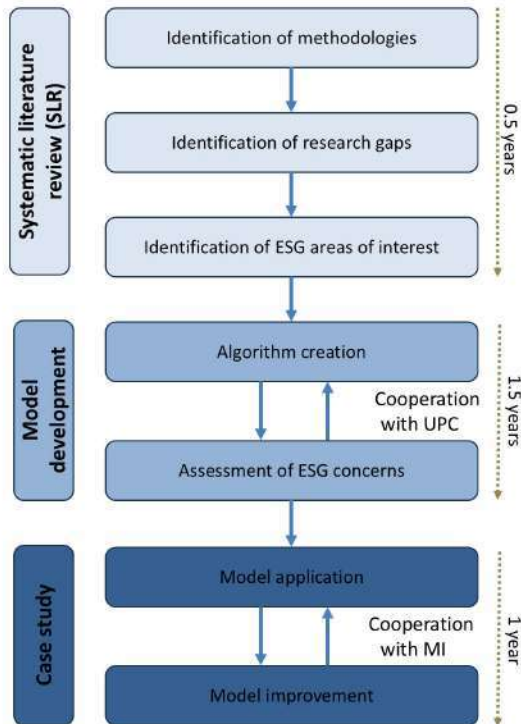


Figure 2. Visual outline of the methodology applied in the project

Expected results

The project is expected to be finalized with the development of a **practical stochastic algorithm** that expands the current, economy-focused solutions and helps mitigate the adverse socio-environmental impacts of mining operations.

References

- [1] Aghdamigargari, M., Avane, S., Anani, A. and Adewuyi, S.O., 2024. Sustainability in long-term surface mine planning: a systematic review of operations research applications. *Sustainability*, 16(22), p.9769.
- [2] Dimitrakopoulos, R., 2018. Stochastic mine planning—Methods, examples and value in an uncertain world. In *Advances in Applied Strategic Mine Planning* (pp. 101-115). Cham: Springer International Publishing.
- [3] Levinson, Z. and Dimitrakopoulos, R., 2020. Simultaneous stochastic optimisation of an open-pit gold mining complex with waste management. *International Journal of Mining, Reclamation and Environment*, 34(6), pp.415-429.

AI Application for Prediction of Deep Underground Mine Excavation Instability: a Comparative Study to Geomechanical and Numerical Modelling Methods

PhD. Mining and Geo-Resources Engineering

Oludare Joseph, Olufe (up202200543@edu.fe.up.pt)

Supervisors: Maria De Lurdes Dinis and Antonio Topa Gomes

Background:

The exponential surge in global demand for metals and minerals has compelled modern underground mining operations to excavate at increasingly greater depths in order to meet this growing demand. Stable and rising metal prices, together with advances in mining technology, have made ultra-deep mining both technically feasible and economically viable at depths exceeding 1,500 m below the surface. As underground mines extend to greater depths, the challenges of excavation instability increase significantly.

Excavations in deep mines are subjected to high in situ stresses, which when combined with geomechanical, operational, and environmental factors, substantially increase the likelihood of rock falls, rock bursts, and roof collapses. Such incidents frequently result in damages to costly mining equipment, injuries to mine workers, and, in severe cases, loss of life. In certain instances, excavation instability has led to the complete collapse and closure of mine sections, resulting in loss of access to substantial mineral reserves. These outcomes consequently impose significant negative economic impacts, potentially rendering mining operations unprofitable and leading to business failure.

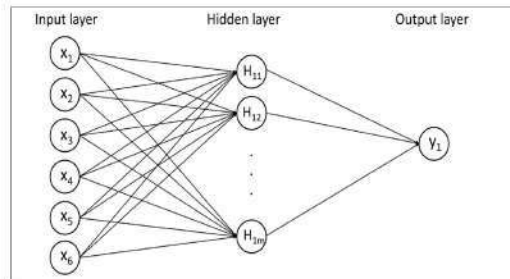


Figure 3: Artificial Neural Networks (ANN) architecture (Source: Keawsawavong et al., 2022)

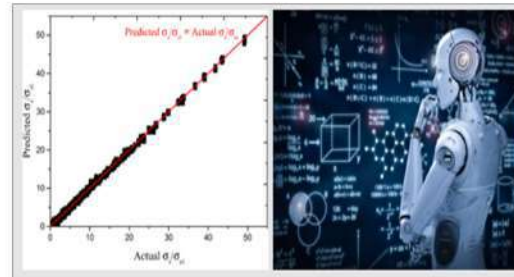


Figure 4: ANN model stability factor prediction results against actual for a rectangular tunnel (Source: Keawsawavong et al., 2022)

Research Goals:

- Deep mine excavations instability prediction
- Improved safety and health of mine workers
- Sustainable extraction of critical metals and minerals
- Economic viability of deep and ultra deep mining operations

Research Methodologies:

- Geomechanical evaluation
- Numerical modelling:
 - Finite element modelling (FEM)
 - Discrete Fracture Network (DFN)
- AI Modelling and Machine learning using:
 - Artificial Neural Networks (ANN)
 - Support Vector Machine (SVM)
 - Random Forest (RF)

Expected Results:

It is anticipated that the application of artificial intelligence (AI), through the use of machine learning (ML) models, can effectively learn from datasets related to rock mass characteristics, excavation geomechanics, excavation design parameters, and mining operational and environmental conditions. Such models are capable of extracting hidden patterns and insights from the complex interrelationships among the influencing factors that contribute to deep underground excavation instability. Consequently, AI-based approaches have the potential to predict excavation failure accurately and in a timely manner, while significantly reducing the computational demands associated with conventional numerical modelling of underground mine excavation stability under complex conditions.

Discussion:

The prediction of underground mine excavation instability is inherently complex due to nonlinear interactions among geological, geomechanical, operational, and environmental factors, and while traditional geomechanical evaluation and numerical modelling techniques have been essential for understanding excavation behaviour, they often rely on simplify assumptions and are computationally demanding, particularly in deep and highly stressed mining environments. In this context, artificial intelligence (AI) and machine learning (ML) approaches could offer a promising alternative, as they are capable of learning complex nonlinear relationships directly from data without explicit formulation of governing physical equations, thereby revealing hidden patterns and interdependencies among multiple influencing parameters and enabling accurate prediction of excavation instability, including rock falls, rock bursts, and roof collapses, when trained on comprehensive and representative datasets.

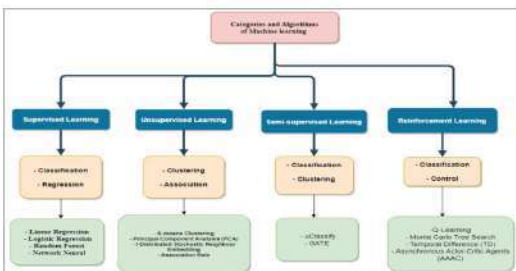


Figure 2: Machine learning types, functions, and algorithms (Source: Taye, M. M., 2023)

Enhanced tailing modelling, characterization, and exploration

PhD Programme: Energy and Earth Resources

Amir Afzali (amir.afzali@tecnico.ulisboa.pt)

Supervisors: João Narciso, Leonardo Azevedo

Objectives

- Develop drone-based geophysical methods for safe mine tailings characterization.
- Automate real-time geophysical inversion using deep learning.
- Test and validate all methods using real field data.
- Design sustainable and optimized strategies for tailings recovery, integrating multiple objectives such as excavation efficiency, environmental protection, and societal impact.

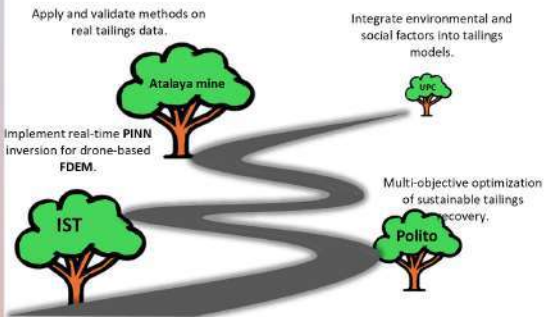


Figure1. Project Timeline: Tasks and International Collaborations

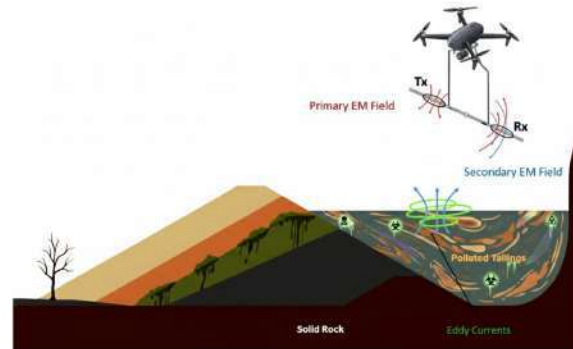


Figure 2. Schematic of a drone-based FDEM survey structure.

Expected results

- Innovative deep-learning methods (PINNs) for geophysical inversion.
- Integrated real-time inversion frameworks to optimize drone navigation and flight paths.
- Multi-objective, data-driven optimization for tailings recovery.

Methodology

1. Real-time inversion: Physical-informed neural networks (PINNs) predict spatial rock properties from FDEM data acquired by drones [1].
2. Adaptive flight planning: Use inversion outputs to optimize drone paths (minimize time and environmental impact).
3. Multi-objective recovery: Stochastic or deep learning optimization to balance excavation, social, and environmental goals.

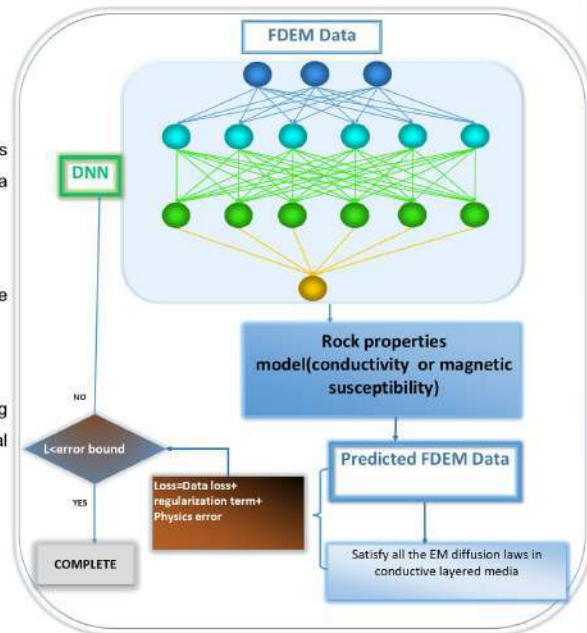


Figure 3. Schematic PINN for FDEM.

References

- [1] Dadras Javan F, Samadzadegan F, Toosi A, van der Meijde M. Unmanned Aerial Geophysical Remote Sensing: A Survey. Preprints 2024. doi:10.20944/preprints202411.0058.v1
- [2] Souza R, Codas A, Nogueira Junior A, et al. Supporting the Training of Physics Informed Neural Networks for Seismic Inversion Using Provenance. AAPG Annual Convention and Exhibition (ACE) 2020. Online/Virtual, Sept 29–Oct 1, 2020.

Acknowledgments

The Criteria project is funded by the European Union under Horizon Europe Marie Skłodowska-Curie Actions - Doctoral Networks (Grant Agreement No. 101169238).

Technosol From Mining Tailings

PhD Mining Engineering and Geo-resources
 Tiago da Costa Silva (up202202395@edu.fe.up.pt)
 Supervisor: Professor Maria Cristina Vila

INTRODUCTION

Mining tailings pose a growing global challenge, presenting environmental risks due to their storage. Technosol offers a potential solution, as its formulations can transform these wastes into usable soil, facilitating their return to nature.

MATERIALS

Technosol formulation to develop from Panasqueira mining tailings.

Amendments:

Compost (organic compost from Wastewater Treatment Station, ETAR de Parada);

Garden soil (a soil from Porto region);

METHODS

Mixed components into treatments.

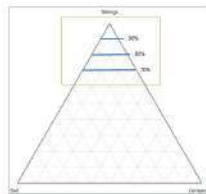
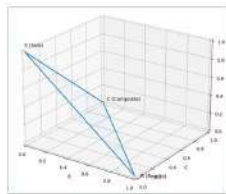
Mixture DoE, 3 components.

x_1 - Mining tailings (70-100%)

x_2 - Compost (0-30%)

x_3 - Garden soil (0-30%)

$$x_1 + x_2 + x_3 = 1$$



Treatments: 9 Formulations + 2 Controls

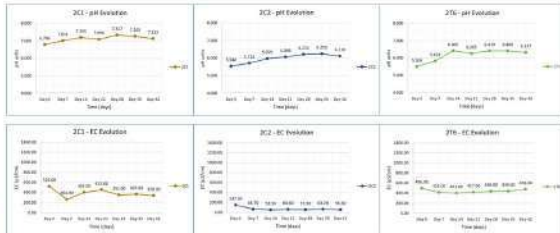
Duration: 42 days

Key Parameters: pH and EC

Treatment	Mining Tailings (%)	Compost (%)	Garden Soil (%)
2T1	90	10	-
2T2	90	-	10
2T3	90	5	5
2T4	80	20	-
2T5	80	-	20
2T6	80	10	10
2T7	70	30	-
2T8	70	-	30
2T9	70	15	15
Control 1	100	-	-
Control 2	-	-	100

RESULTS

pH and EC monitoring:

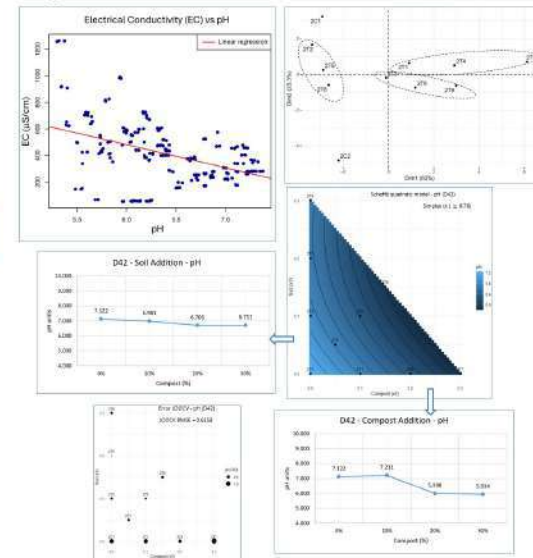


Stability after 14-21 days, pH and EC;

Compost ↓pH and ↑EC;

Soil ↑pH and ↓EC;

Negative correlation; Clustered PCA;



CONCLUSION

Modeling can reduce costs and time.

Potentially better results:

Mining tailings 70-80%

Compost 10-20%

Garden soil 10-15%

ACKNOWLEDGMENTS

This research, part of a doctoral thesis at FEUP in Porto, Portugal, has benefited from support by the Instituto Federal da Paraíba (IFPB), Campus Picuí.

Hydroconversion of advanced non-conventional feedstock: impact of co-processing

Chemical Engineering PhD programme (DEQuim)

Arij Ben Hassine (arij.ben.hassine@tecnico.ulisboa.pt)

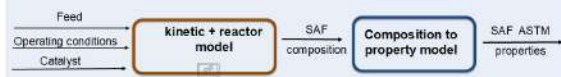
Supervisors: Pedro S.F. Mendes; M. Joana N. Correia

Introduction

Co-processing renewable feedstocks is a promising route to Sustainable Aviation Fuels (SAF). This work models mixture effects in used cooking oils (UCO) and lignin-derived pyrolysis oils hydro-processing.



Methodology



Experimental work is performed in parallel to validate the kinetic and reactor model.

Reaction network

Representative molecules were used for modeling: oleic acid for used cooking oil, and guaiacol for lignin-derived bio-oil.

Hydrogenation to aldehyde:



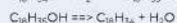
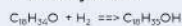
Decarboxylation:



Decarbonylation:



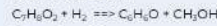
Direct dehydration:



Oleic acid



Demethoxylation



Ring saturation



Dehydration



Demethylation



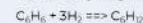
Dehydration of catechol



Phenol hydration to benzene



Benzene hydrogenation



Guaiacol



Results

Kinetic + reactor model

Predictions accuracy was tested with available experimental data (R. Chanakya (2019)).

Good prediction accuracy for OA as an individual feed and as a mixture with Guaiacol (Figure 1a-b). Aromatic molecule validation gave some deviations due to missing data and will be further refined using our own experimental data.

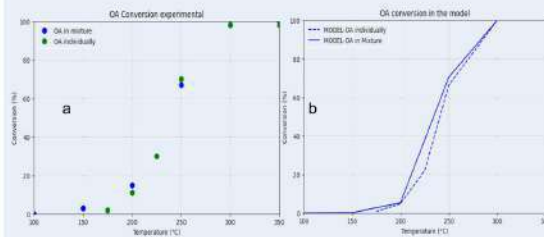


Figure 1: Experimental data (a) vs Model predictions (b) (R. Chanakya (2019)), for Oleic Acid (OA) processed individually and in mixture as a function of temperature at 6 MPa.

Composition to property model

Supervised machine learning was applied screening various regression methods. Non-linear methods (e.g. Scheffé) have shown good accuracy for properties exhibiting nonlinear behavior regarding composition (e.g. KV (figure 2.a)) while linear methods (e.g. PLS) gave better accuracy for properties with non-linear behavior (e.g. NHC (figure 2.b)).

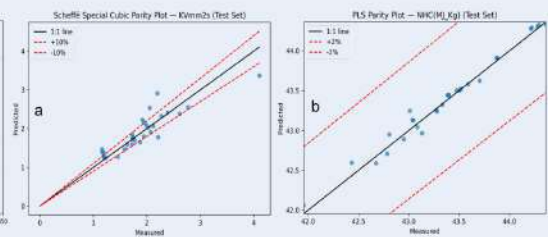


Figure 2 Predicted vs observed values of (a) Kinematic viscosity using scheffé-special cubic and of (b) Net heat of Combustion using PLS.

Conclusions

This work provides a simulation tool linking feed properties to final SAF specifications supporting flexible co-processing. The kinetic model captures key mixture effects observed experimentally with further experimental investigation required for Guaiacol. The composition to property model showed high prediction accuracy when appropriate method was applied to each property.

Acknowledgments

Centro de Química Estrutural is a Research Unit funded by Fundação para a Ciência e a Tecnologia through projects UIDB/00100/2020 and UIDP/00100/2020. Institute of Molecular Sciences is an Associate Laboratory funded by Fundação para a Ciência e a Tecnologia through project LA/P/0056/2020. Agenda Moving2Neutrality n.º C644927387-00000038, projeto n.º 32.

Sol-Gel Synthesis and Catalytic Performance of Zr-P Catalysts

PhD in Materials Sciences@Faculty of Sciences Ibn Tofail

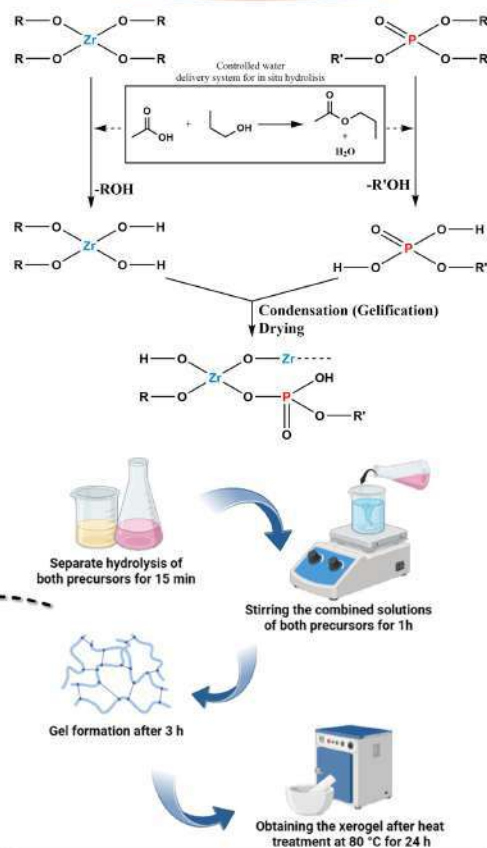
Salma Dehhaoui (salmadehhaoui@tecnico.ulisboa.pt)

Supervisor: Rui Galhano dos Santos

Background

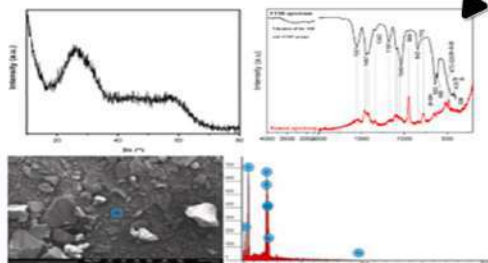
Zirconium phosphates are versatile materials used in catalysis, separations, and fuel cells. Their combined Brønsted-Lewis acidity in $ZrO_2-P_2O_5$ enables efficient multicomponent reactions. This study focuses on synthesising a $ZrO_2-P_2O_5$ xerogel via the sol-gel process and evaluating it as a heterogeneous catalyst for the efficient, environmentally friendly synthesis of 2,3-dihydroquinazolin-4(1H)-one (DHQs), a class of compounds with significant pharmacological relevance. While both oxide materials and their catalytic applications are well established, the originality of our work lies in the rational design of a $ZrO_2-P_2O_5$ catalyst via a sol-gel co-condensation route.

Xerogel Synthesis



Characterisation

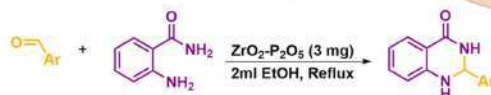
- XRD- crystalline structure
- FTIR- functional groups
- SEM-EDS- Morphology
- Raman- structural features



The xerogel is used as a catalyst for the synthesis of dihydroquinoxalines.

Application

Optimisation of solvent



Optimisation of catalyst load

Entry	Solvent	Time (min)	Yield (%)	Entry	Zr-P (mg)	Time (min)	Yield (%)
1	EtOH	8	93	1	1	8	92
2	MeOH	17	71	2	2	8	92
3	EtOH:H ₂ O (2:1)	30	65	3	3	8	93
4	EtOH:H ₂ O (1:2)	37	55	4	4	7	89
				5	5	7	84
				6	6	7	84

Key Takeaways

- Zr-P xerogel prepared by a simple and straightforward sol-gel method
- Xerogel showed **high catalytic efficiency** under **mild conditions**, **short reaction times**
- **93% yield** was achieved in **8 minutes** consistently
- The Zr-P xerogel catalyst was **reused 5 times** while maintaining activity

Total Plastic Recycling – Hydrocarbons and Beyond Contributions to the Circular Economy

Chemical Engineering PhD

M^a Teresa Nogueira (t.miranda.nogueira@tecnico.ulisboa.pt)

Supervisor Prof. Maria Amélia Lemos

Co-supervisor Prof. Ana Clara Marques

OBJECTIVES

Develop methodologies to extract metals and hydrocarbons from complex recycling waste streams containing plastics, particularly biaxially oriented polypropylene (BOPP) plastics.

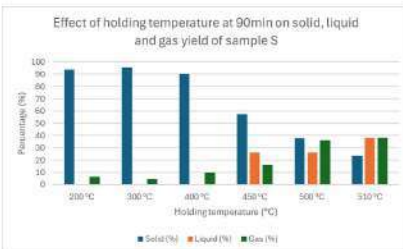
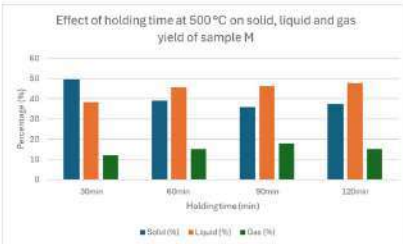
INTRODUCTION

BOPP is a material used in food packaging. It results from the stretching, both longitudinally and transversely, aligning molecular chains in two directions, and a vacuum coating process (metalization, SiO_x, AlO_x). BOPP offers excellent barrier and durability properties. However, because of its multi-layered composition, it poses significant environmental challenges due to the difficulties in its mechanical recycling. Advanced recycling techniques, such as pyrolysis and chemical recycling, show promise in effectively processing these materials back into reusable raw materials, addressing the limitations of traditional recycling approaches, and reducing environmental impact.

METODOLOGY

HYBRID REACTIVE
DESTILLATION (HyRD)
Lab-scale reactor (pyrolysis)

Sample S = Wrapper for chocolate-covered biscuits
Sample M = Wrapper for chocolate bar



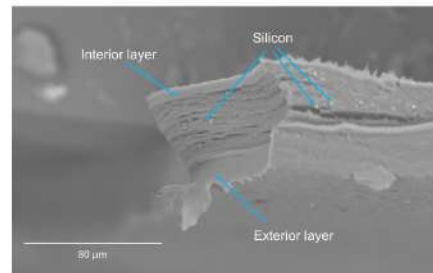
BOPP example
Chocolate wrap



✓ Polypropylene plastic packaging

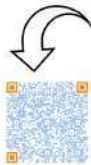
✗ Cannot be recycled
Instructions to dispose in trash

BOPP with silicon oxide

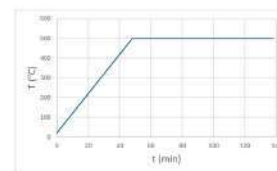


SEM image of sample M.

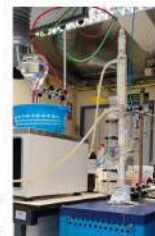
See degradation happening



Goal:
Liquid + Gas



Setup of the lab-scale reactor. Adapted from Santos (2018).



CONCLUSIONS

- About 10% of the reactor's solid residue consists of an inorganic component.
- GC analysis of the reactor's liquid and gaseous residues shows both are composed of hydrocarbons.
- The gas phase contains hydrocarbons between C₂ and C₆, while approximately 80% of the liquid phase consists of hydrocarbons between C₅ and C₁₀ in both samples.
- The best outcome for the HyRD was 500 °C holding temperature and 90 min holding time.
- Pyrolysis is a promising technique for recycling BOPP plastics.

ACKNOWLEDGEMENT

The author would like to thank FCT for the PhD grant (ref UI/BD/154131/2022) and UID/04028 of the CERENA – funded by FCT, I.P./ MECI through the national funds).

REFERENCE

- [1] Catafati, T. (1998). Polypropylene Films. *Elsevier eBooks*, pp.17–20. <https://doi.org/10.1016/b978-1-4557-3112-1.00002-8>.
- [2] Breil, J. (2016). Oriented Film Technology. *Elsevier eBooks*, [online] pp.153–172. <https://doi.org/10.1016/b978-0-323-37100-1.00012-0>.
- [3] Breil, J. (2013). Biaxially Oriented Films for Packaging Applications. *Elsevier eBooks*, pp.53–70. <https://doi.org/10.1016/b978-1-4557-3112-1.00004-1>.
- [4] Santos, E., 2018. *Nanostructure Materials as Catalysts for the Degradation of Polyolefins*.

Bio-oil from Biomass: Mapping Fuels and Forest Management

Chemical Engineering

Ana Raquel Gonçalves (raquel.goncalves@tecnico.ulisboa.pt)

Supervisors: Rui Galhano dos Santos, Sandra Heleno, Gabriel Goyanes

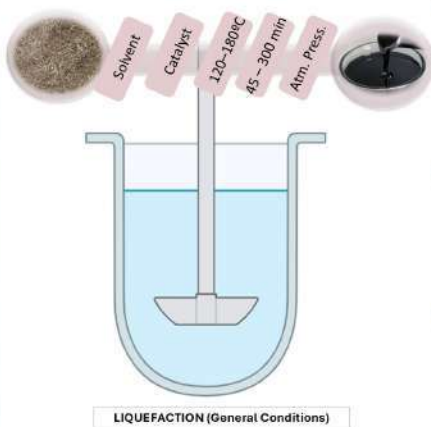
Objectives

Precision Fuel Mapping: Employ high-resolution drone imagery to identify the distribution, quantity, and moisture content of dry vegetative biomass.

Sustainable Bio-Oil Production: Utilize thermochemical liquefaction to transform harvested biomass into bio-oil, enhancing its potential for renewable energy applications.

Optimized Biomass Utilization: Combine geospatial fuel data with energetic characterization to improve biomass management strategies and mitigate wildfire risks.

Solvothermal Liquefaction



- **Forest biomass was processed through solvothermal liquefaction**, a subcritical thermochemical method that depolymerizes lignocellulosic material into two main products: **bio-oil** and **carbon-rich solid residues**. Reaction conditions (temperature, solvent, residence time) were adjusted to optimize yields and evaluate species-specific behavior.
- **Bio-oil was analyzed for its High Heating Value (HHV)** to assess its energy potential and compare performance across shrub species. Observations on viscosity, phase separation, and composition helped clarify the suitability of Serra da Estrela shrublands as feedstocks for decentralized renewable-energy production.
- **Solid residues were characterized for potential valorisation**, focusing on physicochemical properties, carbon content, and structural stability. Their attributes support applications such as **soil amendment** or **lightweight material supports**, contributing to circular bioeconomy strategies that link fuel-load reduction with value-added products.

Fuel Maps generation with drones

- **Multispectral UAV flights produced high-resolution DTMs/DSMs**, enabling detailed mapping of vegetation structure, fuel height, and fuel load in Serra da Estrela.
- **Species were identified using an SVM classifier**, improving the accuracy of shrub-fuel mapping at fine spatial scales.
- **Classified areas were converted into biomass estimates** using species-specific allometric data, moisture content, and field-measured density.
- **Fuel maps were validated with ground-truth biomass measurements**, ensuring consistency with material available for thermochemical liquefaction.
- **Biomass volumes were combined with species-specific HHV values**, generating **spatial energy-potential maps** that highlight areas with higher renewable-energy value.
- **These maps support biomass management and wildfire-risk planning**, linking remote-sensing fuel assessments with energetic performance.



Conclusions:

This workflow demonstrates how combining UAV-based vegetation mapping, automatic classification, and bio-oil energy profiling can enhance forest biomass utilization and contribute to fire prevention strategies. The resulting fuel maps offer a valuable tool for both ecological monitoring and renewable energy planning.

[1] Fernandes, F.; Matos, S.; Gaspar, D.; Silva, L.; Paulo, L.; Vieira, S.; C. R. Pinto, P.; Bordado, J.; Galhano dos Santos, R. Boosting the Higher Heating Value of Eucalyptus Globulus via Thermochemical Liquefaction. *Sustainability* 2021, 13, 1717. doi:10.3390/su13071717.

[2] Zhao, Y.; Liu, X.; Wang, Y.; Zheng, Z.; Zheng, S.; Zhao, Q.; Bai, Y. UAV-Based Individual Shrub Aboveground Biomass Estimation Calibrated against Terrestrial LiDAR in a Shrub-Encroached Grassland. *Int. J. Appl. Earth Obs. Geoinformation* 2021, 101, 102358. doi:10.1016/j.ijag.2021.102358.

Performance, prediction and optimization of green hybrid composites for additive manufacturing in industrial applications: experimental and machine learning (ML) studies

PHD in Materials Engineering

Rita M. N. Serôdio (rita.serodio@tecnico.ulisboa.pt)

Supervisor Prof. Célio Pina, Prof. Ana C. Marques, Prof. Pedro Mendes

Introduction

Increasing concern regarding the environmental impact of plastic waste in the earth's ecosystem and human health motivates the transition towards a 'circular plastic economy', transitioning towards bioplastics [1–5].

Bioplastics are a class of materials that are either bio-based, biodegradable or both [2, 3]. Our focus is on the use of bioplastics reinforced with **natural fibers** derived from a second-generation biomass waste, to innovatively reuse agro-industrial residues [2, 3, 6, 7]. In particular, a promising area of research is **green hybrid composites** that allow to strategically combine these elements for new and improved combinations of materials [8]. When used in the automotive industries it can promote weight reduction, and consequently less fuel consumption and greenhouse gas emissions [9, 10].

Meanwhile, **Artificial Intelligence (AI)**, particularly supervised **Machine Learning (ML)**, enables the in silico optimization of material properties [11] and guides polymer design, which is especially valuable for hybrid composites with numerous possible formulations. To the best of our knowledge, the use of ML to design green hybrid composites has not been yet explored. Therefore, this project aims to fill this gap and substitute this trial-and-error process into a data-driven, model framework of ML algorithms for **Fused Deposition Modeling (FDM)** of green hybrid composites with tailored characteristics for innovative automotive applications.

Methodology, Results and Future applications

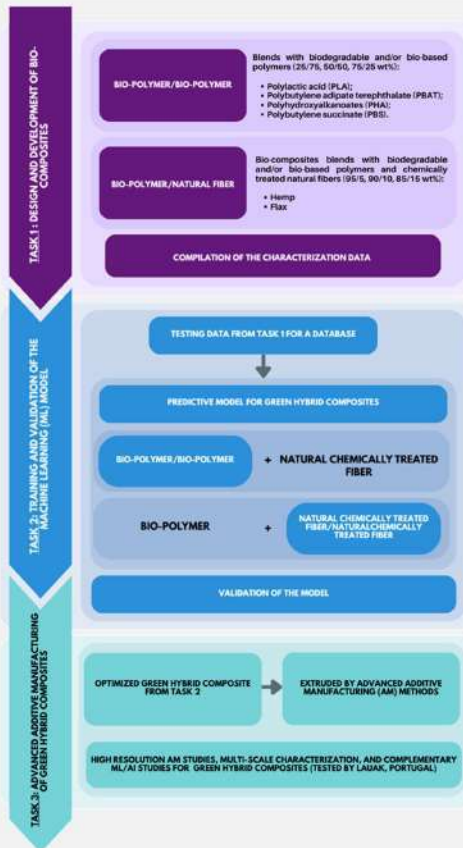


Table 1 – Results for Dynamic Mechanical Analysis (DMA), Thermogravimetric Analysis (TGA) and Differential Scanning Calorimetry (DSC) of bio-polymers and their composites

Bio-polymers and Composites	DMA		TGA	DSC	
	E' (GPa)	Tg (°C)	T _{onset} (°C)	T _m (°C)	χc (%)
PBAT	3.2	-21	385	123	8
50PBAT/50PBS	3.9	-21	383	116	-
PBS	5.1	-18	380	118	71
50PBS/50PLA	6.1	-20 51	329 394	115 175	38 15
PLA	6.8	61	337	174	33
50PLA/50PHB	5.5	8 51	289 347	141 156	4 19
PHB	7.2	13	284	169	43



Figure 1 – Automobile parts produced from bio-based material in the Lexus CT200h. Reprinted from [12], with permission from Wiley.

Acknowledgements: This research was funded by FCT (Fundação para a Ciência e Tecnologia) under the scholarship 2025.04146.BD, CERENA, Strategic Project FCT-UIDB/04028/2025 and FCT-UIDP/04028/2025, and Talent Pass, Grant Agreement No. 10121448 – HORIZON-WIDERA—TALENTS-03.

References

- [1] J. B. de Lencastre, A. Reder, S. Sengupta, S. Shin, G. H. & Kim, J. T. (2023). Recent progress of bioplastics in their properties, standards, certifications and regulations: A review. *Science of the Total Environment*, 878, 163155. doi: 10.1016/j.scitotenv.2023.163155. (2) B. B. de Lencastre, J. G. Langer, R. & Travenço, G. (2022). Bioplastics for a circular economy. *Integrative Reviews Materials*, 7(2), 117-137. doi: 10.1039/1157821-00487.5. [3] R. P. M. de Lencastre, S. Pina, S. G. G. de Lencastre, E. & Sharma, S. K. (2021). Recent advances in the sustainable design and applications of biodegradable polymers. *Bioresour. Technol.*, 320, 124759. doi: 10.1016/j.biortech.2021.124759. [4] A. Reder, G. M. de Lencastre, A. P. de Lencastre, C. C. de Lencastre, J. S. de Lencastre, T. A. T. (2022). Environmental impact of bioplastic use. *Review. Environ.*, 1(2), 10.1016/j.renenv.2021.08.019. [5] M. A. S. de Lencastre, et al. (2023). Bioplastic production in terms of life cycle assessment: A state-of-the-art review. *Environmental Science and Technology*, 57, 10224. doi: 10.1021/acs.est.2c03024. [6] (D. de Lencastre, et al. (2022). Natural and industrial wastes for sustainable and renewable polymer composites. *Renewable and Sustainable Energy Reviews*, 161, 112044. doi: 10.1016/j.rser.2021.112044. [7] E. de Lencastre, F. E. de Lencastre, M. A. S. de Lencastre, A. & B. de Lencastre. (2020). A review on the use of agro-industrial residues in the reinforcement of polymer composites. *Composites Part A: Applied Science and Manufacturing*, 128, 106677. doi: 10.1016/j.compositesa.2019.106677. [8] D. de Lencastre, J. E. de Lencastre, M. A. S. de Lencastre, P. (2023). Machine learning based prediction of polymer and processing related polymer properties: A comprehensive review. *ACS Applied Materials & Interfaces*, 14(38), 42771-42799. doi: 10.1021/acsami.2c08301. [9] M. de Lencastre, D. de Lencastre, P. M. de Lencastre, L. W. & O. X. H. (2017). Review of the applications of biocomposites in the automotive industry. *Polymer Composites*, 38(1), 255-299. doi: 10.1002/polb.23947.

Dissolving the Problem: Plastic Recycling using Natural-Based Solvents

PhD in Chemical Engineering

Sofia C. Aparício (sofia.c.aparicio@tecnico.ulisboa.pt)

Supervisors: Isabel M. Marrucho, Rui Galhano dos Santos

The Plastic Waste Problem



Global plastic production is expected to surpass **500 Mt** in the coming years [1].

Polyolefins comprise over **40%** of the global plastic consumption.

Less than **15%** of all end-of-life polyolefins are recycled.



Common recycling method – **mechanical recycling**

– faces strong **drawbacks**:

- Fails to handle mixed plastics;
- Is unable to remove additives and contaminants;
- Leads to downcycling of even pure single polymer materials.

Dissolution-precipitation recycling is a promising solution for recycling polyolefins:

- In can separate multipolymer materials;
- It can remove additives and contaminants;
- The material is recovered with good quality.



Dissolution-Precipitation: SWOT Analysis

Strengths

Complex materials are separated and recovered with high purity and quality, retaining their added value.

Simple process, involving few steps and inputs.

No degradation sources, except for the mild heating step.

Weaknesses

Higher cost compared to mechanical recycling.

Can require high solvent amounts, that needs to be recovered to ensure economic viability.

Might require an antisolvent, adding to the costs.

Opportunities

Global plastic production increases daily.

Increased regulations boost the need high-quality recycling of end-of-life plastics.

Instability in the petroleum market increases demand for plastic recycling.

Threats

Polymer-to-monomer recycling, although more complex and costly, can be considered more versatile by some market sectors.

Extra tests might be needed to regulate the application in food and cosmetic industries.

Fig. 1 | SWOT analysis of dissolution-precipitation for plastics recycling (adapted from [2]).

Moving Towards Green Solvents

Solvent selection is key when developing dissolution-precipitation processes. It impacts the performance of the process in several aspects:

- **Selectivity**;
- **Operating conditions**;
- **Quantitative polymer recovery**;
- **Solvent recyclability**;
- **Quality** of the recovered materials;
- **Sustainability** of the process as a whole.

Dissolution-processes were developed and optimized:

From a list of natural occurring terpenes, limonene, α -pinene, and *p*-cymene [3] were predicted to correspond to the highest HDPE solubility.



Experimentally, it was confirmed that these were good HDPE solvents, with the best results being attained when using α -pinene. This was selected to test PP dissolution.



Recyclate Characterization

The recyclates obtained from dissolution-precipitation experiments were analyzed regarding:

- Chemical and structural integrity (FTIR)
- Thermal properties (DSC)
- Solvent presence and thermal degradation behavior (TGA).

All PP samples **were recovered with high quality**: there were no solvent traces and all main properties were maintained equal to the pristine materials.

Dissolution-precipitation of polypropylene:

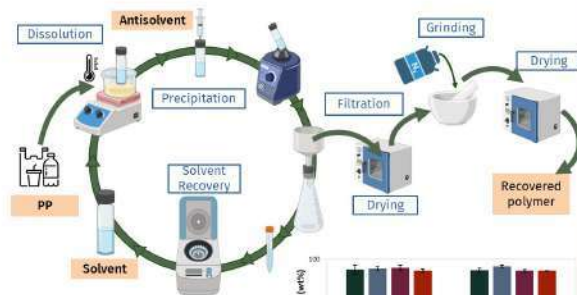


Fig. 2 | PP's dissolution-precipitation process.

It was possible to recycle three different types of PP sample, achieving **high recovery yields** for both the polymer and the solvent used.

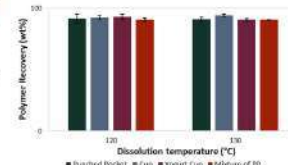


Fig. 3 | PP's recovery yields.

Conclusion

Dissolution-precipitation is a promising technology to **handle complex plastic wastes**.

It was possible to identify **natural-based solvents** for different polyolefins: HDPE, and PP.

By ensuring careful solvent selection and optimizing important operating conditions, **the developed process attained high polypropylene recovery yield and good recyclate quality**.

References: [1] Plastics Europe. The Circular Economy for Plastics – A European Analysis 2024, 2024. [2] S. C. Aparício, J. V. M. Resende, B. D. Ribeiro, I. M. Marrucho, ChemSusChem 2025, e202500018. [3] S. C. Aparício, P. M. Castro, B. D. Ribeiro, I. M. Marrucho, Green Chem. 2024, 26, 6799–6811.

Acknowledgements: The authors gratefully acknowledge the support of Centro de Química Estrutural – CQE (UID/00100/2025 and UID/PRR/100/2025), Institute of Molecular Sciences – IMS (https://doi.org/10.54499/LA/P/0056/2020), and Centro de Recursos Naturais e Ambiente - CERENA (FCT-UIDB/04028/2025 and FCT-UIDP/04028/2025).

Using BELLHOP3D to understand underwater acoustics and generate artificial data

João Duarte Alcântara Galvão (joao.galvao@tecnico.ulisboa.pt)
Supervisor: Dr. Leonardo Azevedo

Understanding and accurately simulating acoustic propagation in marine environment has huge significance, namely in the context of underwater vehicles and communication. This presents many challenges, considering all the variables and associated uncertainties at play, ranging from physical variables to operation range for communication to budget. With all of this in mind, a computational exploration was undertaken, mainly focused on BELLHOP¹, a beam tracing computational model for predicting acoustic pressure fields in ocean environments.

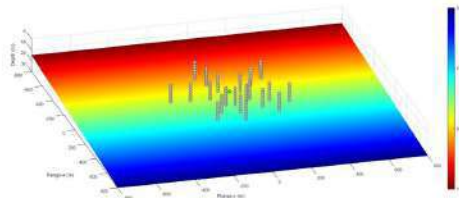


Figure 1: Simulated scenario (ocean bottom, spatial distribution of sound source and receivers, also called hydrophones)

The 3D sound speed profile, along with the source and receivers' location and the bottom's physical properties and geometry, were provided as inputs to the model. The calculated beam trajectories, transmission loss profile and time arrivals are displayed in figures 2, 3 and 4, respectively.

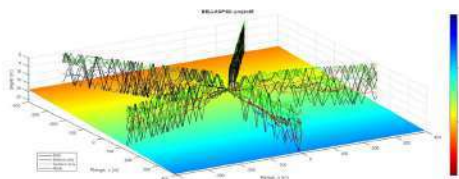


Figure 2: Simulated ray propagation (5 azimuths)

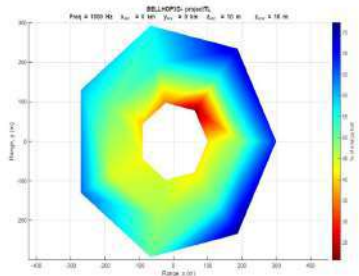


Figure 3: Transmission loss polar profile (fixed depth)

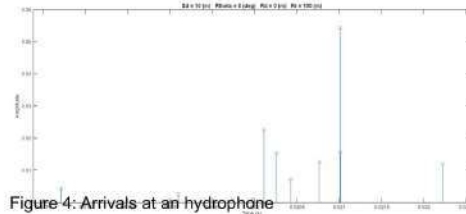


Figure 4: Arrivals at an hydrophone

Convoluting the time arrivals with the source signal waveform leads to arrival time series, exemplified in figure 5.

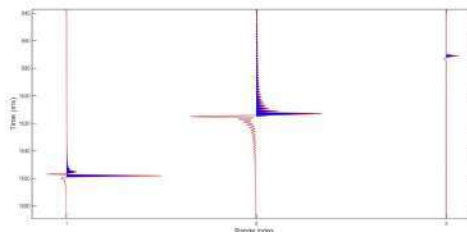


Figure 5: Arrival time series at line of hydrophones (fixed azimuth and depth)

These time series can now be used to perform geophysical inversion on the sound speed profile, interferometric source localization, among other things. Successful prediction of the sound speed profile represents an important step in the understanding and characterization of the ocean for it is directly related to temperature and salinity conditions, whose regimes could be inferred from it. On the other hand, successful localization of a sound source can play a major role in marine biology, underwater communication and defense.

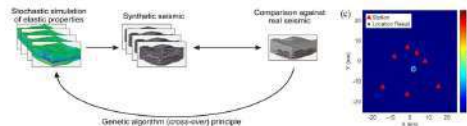


Figure 6: Geophysical inversion - genetic algorithm² (on the left). Interferometric source localization³ (on the right).

References

- Porter, M. B. et al. BELLHOP, Acoustics Toolbox.
- Azevedo, L. and Soares, A. (2017). Geostatistical Methods For Reservoir Geophysics. Springer Cham.
- Zhang, C. et al. (2026). Locating Tremor Using MLE-Based Iterative Peeling Interferometric Imaging. EAGE abstract.

Geomathematical Assessment of Environmental Degradation in Abandoned Mining Areas

Doctoral Programme in Mining Engineering and Geo-Resources, FEUP, Porto
 Bárbara Fonseca | barbarardafonseca@gmail.com

Joaquim Góis (FEUP); António Guerner Dias (FCUP), Henrique Garcia Pereira (IST)

INTRODUCTION

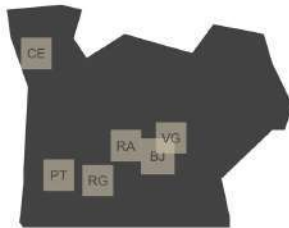
Portugal contains 384 abandoned W-Sn mining explorations within the Portuguese Metallogenic Tin-Tungsten Province, generating severe environmental and public health impacts. Soil contamination by potentially toxic elements (PTE) – particularly As, Zn, Sn, Cu, and W – results from the oxidative weathering of sulfide minerals exposed in abandoned mine tailings and waste dumps.

The main objectives is to assess the environmental impact from potentially toxic elements (PTE) within the Tin-Tungsten Metallogenic Province, employing geomathematical tools to analyze PTE dispersion and accumulation, and focus on representative case studies that capture diverse geological and historical mining contexts within based on predefined criteria.

METHODOLOGY

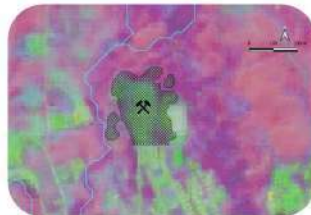
Case Study Selection:

- Binary Correspondence Analysis for case study selection.



Sample Collection Procedures:

- Satellite images to establish sampling grid;
- 214 soil samples collected



Laboratory Analysis:

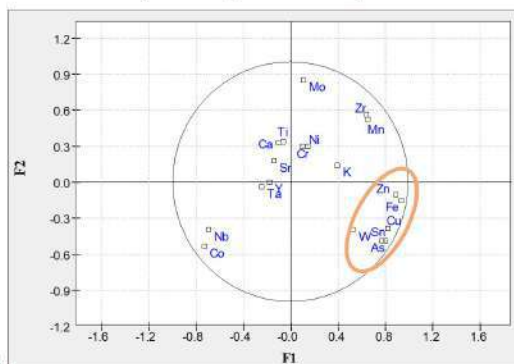
- Sequential XRF;
- XRD;
- Physicochemical characterization



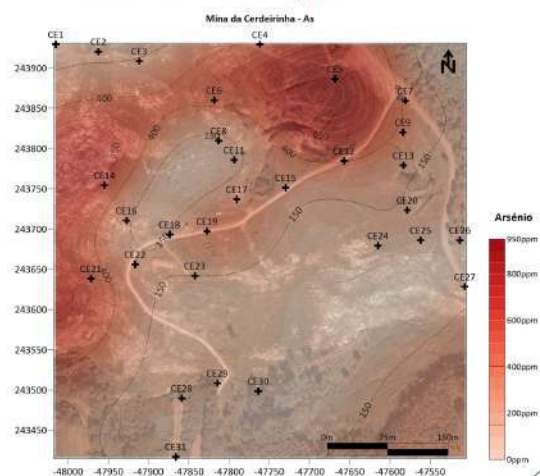
DATA ANALYSIS

Statistical Methods:

- Univariate Statistic Analysis;
- Principal Component Analysis.



Geostatistics Analysis



RESULTS & FINDINGS

- The methodology used to define the areas to be sampled was validated;
- Strong Fe–Zn–Cu–Sn–W clustering in the PCA confirms the expected sulfide paragenesis;
- Multivariate analysis validates the known mineral associations.

Photos



Photos





CERENA

Centro de Recursos
Naturais e Ambiente

Thank you for your
participation in the first
CERENA PhD Day. We
hope to see you again
next year!